THE MÖSSBAUER EFFECT IN FE^{57}

by

Kenneth A. Smee, B.Sc.

A thesis submitted to the Faculty of Graduate Studies and Research in partial fulfilment of the requirements for the degree of Master of Science.

Eaton Electronics Research Laboratory
McGill University
Montreal

April 1964

TABLE OF CONTENTS

ACKNOWLEDGEMENTS

The writer wishes to express his sincere thanks to Professors G.A. Woonton and J. F. Mathison for their guidance during the course of this work.

He also wishes to express his gratitude to G. L. Dyer for his active help in the building of the Mössbauer effect equipment, and for many stimulating discussions.

The writer also wishes to thank Mr. V. Avarlaid and his staff, who made many parts of the equipment.

He finally wishes to acknowledge his indebtedness to the National Research Council for financial assistance in the form of one Bursary and one Studentship.

ABSTRACT

Apparatus has been designed and constructed which detects the Mössbauer effect in Fe^{57} at room temperature. The effect has been studied in detail with various source and absorber combinations: the sources being Co^{57} in copper, 310 stainless steel and iron; and the absorbers being natural iron, enriched Fe^{57}, and 310 stainless steel 0.001 inch thick and 0.00015 inch thick. The theory of the Mössbauer effect is reviewed briefly.

The mean lifetime of the first excited state of Fe^{57} is found to be at least 0.61×10^{-7} secs. The isomer shift detected in one of the source-absorber combinations indicates that the nuclear charge radius for the first excited state of Fe^{57} is smaller than that for the ground state of Fe^{57}. The excited state and ground state splittings of Fe^{57} are found to be 1.04×10^{-7} ev and 1.86×10^{-7} ev, respectively. The internal field at the iron nucleus is 3.28×10^{5} oe, and the magnetic moment of the first excited state of Fe^{57} is (-)0.152 nm.

As a result of the information and experience gained, recommendations for future Mössbauer effect research are made.

CHAPTER I

INTRODUCTION

The discovery by R.L. Mössbauer [1] that gamma ray emission could take place without an associated nuclear recoil when the decaying atom is bound in a crystal lattice has given physicists a valuable new experimental tool. When this bound atom emits a gamma ray, the crystal as a whole recoils. However, because of the large mass of the recoiling crystal, the energy associated with the recoil is negligibly small. As a result, the emitted gamma ray has an energy very close to that of the nuclear transition, making possible resonance absorption. It is the extreme narrowness of the line-width of these gamma rays (4.70×10^{-9} ev for Fe^{57}) which makes the Mössbauer effect so important.

The Mössbauer effect is observed by measuring the transmission in an absorption experiment in which the source and absorber can be given definite relative velocities. This velocity produces a Doppler shift in the gamma energy which, for sufficiently high velocities, destroys the resonance absorption. The transmission thus indicates the Mösbauer effect by a minimum in the counting rate as a function of the velocity.

Although the Mössbauer effect itself belongs in the category of nuclear physics, many of its applications are investigations of solid-state properties. As a preliminary to the application of the effect to obtain phonon spectra, a study was thought necessary of the Mössbauer effect in Fe^{57}

using various source and absorber combinations. It is this investigation which forms the basis of this thesis.

In order to discuss the Mössbauer effect in more detail, resonance absorption must first be considered. Consider a free atom with two energy levels A and B separated by an energy E_r. If the atom decays from B to A by emitting a gamma ray of energy E_γ, momentum conservation requires that the momentum of the gamma ray be equal and opposite to that of the recoiling atom. Therefore, the recoiling atom of mass M receives an energy

$$R = \frac{E_\gamma^2}{2Mc^2} \qquad (1\text{-}1)$$

Thus the total transition energy is related to the gamma energy by

$$E_r = E_\gamma + R \qquad (1\text{-}2)$$

Suppose state B has a mean lifetime τ. According to the Heisenberg uncertainty principle, the energy can only be measured within an uncertainty given by

$$\tau \cdot \Gamma = \hbar \qquad (1\text{-}3)$$

Therefore the energy of state B is represented by a distribution of line-width Γ, centered about E_r and the gamma rays emitted in the transition from B to the ground state A are represented by a distribution centered about $E_\gamma = E_r - R$.

When a photon of energy E_γ strikes an identical target atom which is initially at rest, the momentum of the photon is transferred to the target, causing it to recoil with a kinetic energy R. Thus the gamma ray is left with an energy $E_r - R$. However, for resonance absorption to occur, the gamma must have

the complete transition energy E_r. Therefore the incoming gamma ray must have an energy E_r+R.

As a result there is an energy deficit of 2R between the emitted and resonantly absorbed photons.

Only the overlapping part of the distributions is responsible for resonance absorption. From Figure 1-1 it can be seen that the overlap condition is $2R \lesssim \Gamma$. Optical transitions fulfill the condition (d), but nuclear transitions do not, (e).

The emitting and absorbing systems were assumed to be at rest initially. Actually, however, the source and target atoms are in thermal motion, and this motion introduces an additional widening of the emission and absorption energy distributions called Doppler broadening.

For optical radiation the Doppler broadening is large compared to the recoil energy R and so plays an important role.

However, for nuclear gamma rays the recoil energy is comparable to, or greater than the Doppler broadening.

Therefore, for a resonance absorption experiment to be possible with gamma rays, the recoil energy R must either be compensated for, or somehow made very small ($2 \lesssim \Gamma$).

The devices which were used to observe nuclear resonance absorption before Mössbauer's discovery all supplied in some way the 2R difference between the energy of the emitted gamma ray and the energy it needed to be absorbed.

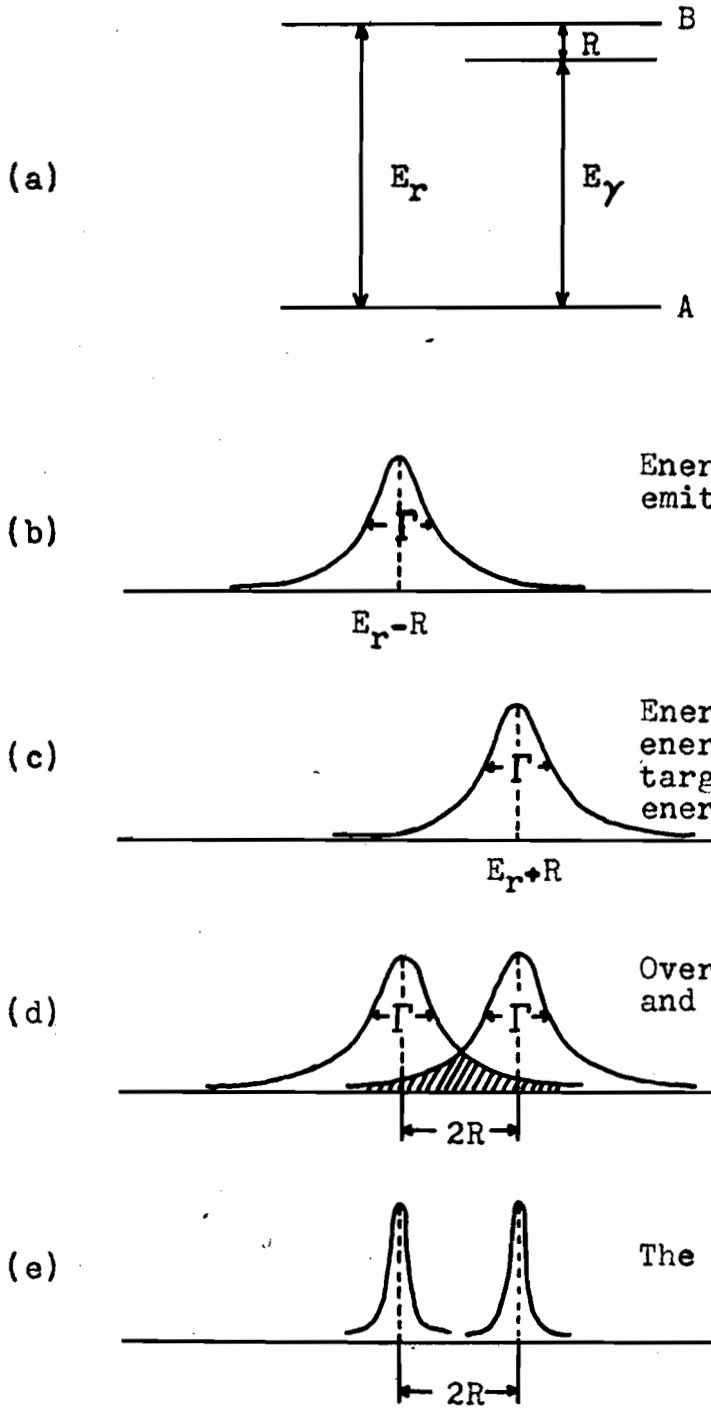

FIGURE 1-1 ENERGY LEVELS AND DISTRIBUTIONS

Moon [2] made use of the Doppler effect by mounting the source on a high speed rotor, thus shifting the emission spectrum towards the absorption spectrum of the stationary absorber.

Another method used by Swann and Metzger [3] uses as a source a nucleus which is recoiling from a previous decay. The decay product is required by coincidence techniques to be travelling in a certain direction with respect to the direction of the subsequently emitted gamma ray, thus fixing the component of velocity of the nucleus along that direction and the Doppler shift in the energy.

Malmfors [4] heated the source so as to spread the emission spectrum by Doppler broadening, thereby increasing the overlap with the absorption spectrum.

It was while investigating the method used by Malmfors that Mössbauer made his discovery. He was studying the 129 kev transition of Ir^{191} which has a recoil energy small enough and a Doppler broadening large enough to cause sufficient overlap to observe resonance scattering. Since the Doppler broadening is caused by thermal motion of the source and target atoms, Mössbauer cooled both the source and absorber, thinking this would reduce the broadening and thus the resonance scattering. Instead, however, he found that the resonance scattering was increased.

After confirming that the increase actually did exist, Mössbauer explained it by adapting to gamma rays a paper by

Lamb [5] which discussed the effects of lattice binding on the capture cross section of slow neutrons.

When the source was cooled, some of the nuclei were bound in the lattice, and therefore did not show a measurable recoil energy R when the gamma rays were emitted. (Since $R=\frac{E_\gamma^2}{2Mc^2}$, if the source is bound in the lattice, the mass M is very large making R negligible.) Similarly for the cooled absorber. Thus the emission and absorption spectra were undisplaced resulting in a large overlap. Also, since these spectra did not display a Doppler broadening, their line-width corresponds to the natural line-width.

To prove his explanation, Mössbauer carried out two experiments. The first, called the temperature effect experiment, was carried out with both source and absorber at rest. The absorber was held at a fixed temperature of 88° K while the source temperature was varied from 88°K to above room temperature. The transmission of the 129 kev gamma rays through the absorber as a function of temperature was measured (see Figure 1-2). As explained before, the rise in cross section with decreasing temperature is interpreted as being caused by an increase in the probability of no-recoil emission by the nuclei in the source as the temperature is lowered.

In his turntable effect experiment, both source and absorber were kept at 88°K, but the source was mounted on a turntable with the absorber at rest. Thus the emitted gamma rays could be given definite relative velocities. The relative

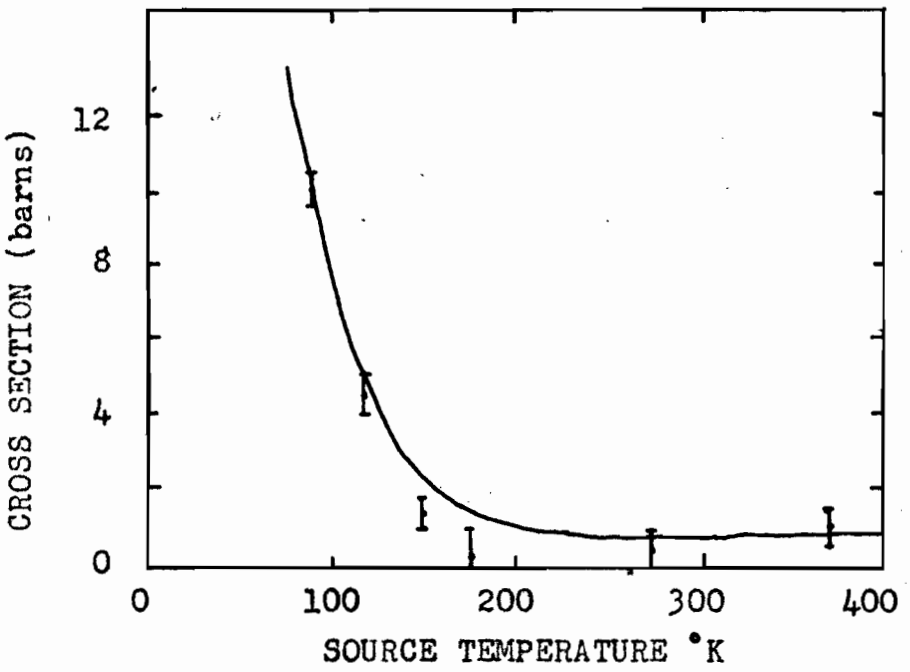

FIGURE 1-2 RESONANCE ABSORPTION vs. TEMPERATURE

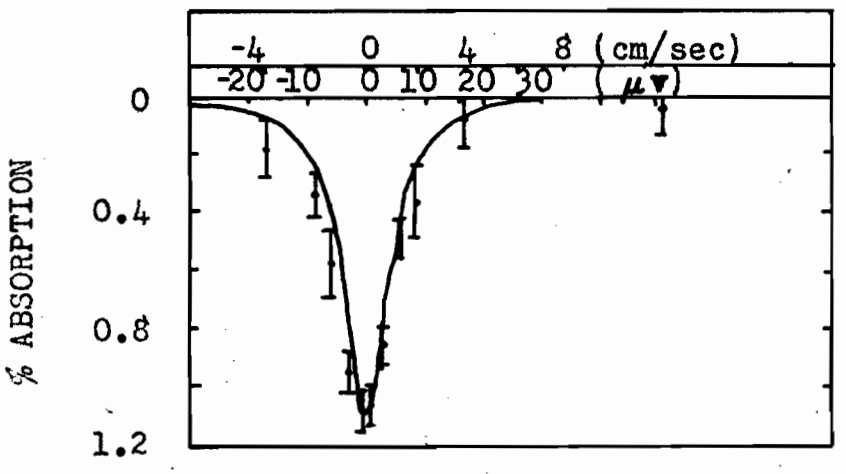

FIGURE 1-3 RESONANCE ABSORPTION vs. VELOCITY

intensity of the 129 kev gamma rays transmitted by the stationary iridium absorber as a function of source velocity was measured.

By converting the Doppler shift due to the source velocity to energy units, a curve is obtained which has a line-width twice that of the natural line-width Γ. The factor of two arises because the observed absorption is the result of "folding" an emission spectrum together with an absorption spectrum, each of which have a line-width Γ. At zero velocity the two spectra overlap, while at high velocities the overlap is destroyed, and resonance absorption disappears (see Figure 1-3).

Mössbauer's results were published in 1958, but were not noticed for a year. When other laboratories began to repeat and extend his experiments, they also used Ir^{191}. These early experiments were complicated by the necessity to work at low temperatures. Also, the effect was quite small.

The discovery in 1959 of the Mössbauer effect in Fe^{57} made independently at Harvard [27], Harwell, [28] the University of Illinois [29], and Argonne [30], was a very important advance.

The effect in Fe^{57} gives a large change in absorption cross section at resonance. The effect persists even up to 1000^{o} C, and the natural line-width is very narrow. This new advance made the Mössbauer effect a much more valuable tool, for it eliminated the low temperature requirement, and gave a large effect. The investigation of the Mössbauer effect reported here was done with Fe^{57}.

CHAPTER II

THEORY

2.1 THE PHYSICAL PICTURE

Mössbauer showed that when the 129 kev gamma ray of Ir^{191} is emitted or absorbed by a nucleus found in a crystal at low temperature, the recoil momentum is taken up a large part of the time by the whole crystal, with no energy transferred to internal excitations of the lattice. The kinetic energy associated with the crystal as a whole is negligible compared to the natural line-width and, as a result, resonance absorption can be observed.

Thus, Mössbauer transitions are characterized by the fact that no energy is transferred to the lattice. In order to see that this is possible the physical picture will now be considered. This physical picture treatment follows fairly closely that given by Frauenfelder,[6] (p.20).

2.11 MOMENTUM CONSERVATION

Assume that the nucleus of an atom which is embedded in a solid decays by gamma emission. If free, the nucleus would receive recoil momentum and recoil energy. How does the binding of the atom in the solid affect the recoil momentum?

There are three possible ways the momentum could be taken up: translational motion of the nucleus, phonons (lattice vibrations), or by the solid as a whole.

The momentum cannot go into translational motion of

the nucleus. The energy required to leave a lattice site is at least of the order of 10 ev, while the recoil energy never exceeds a few tenths of an ev.

Also, the lattice vibrations cannot take up momentum. They can be represented as standing waves or as the sum of running waves. To each wave with its momentum pointing in one direction there will be a corresponding one with its momentum pointing in the opposite direction. Thus, the expectation value of the momentum for lattice vibrations vanishes, and there is no transfer of momentum in a crystal vibration.

Therefore, the momentum must go into translational motion of the entire crystal.

2.12 ENERGY CONSERVATION

Again, assume that the nucleus of an atom which is embedded in a solid decays by gamma emission. Consider how binding the atom in this solid will affect the recoil energy.

If the atom is bound in a solid, the transition energy can be shared among the gamma ray, the individual atom, lattice vibrations, and the solid as a whole. The individual atom does not leave its lattice site and hence cannot acquire translational energy. The energy that goes into motion of the entire solid is extremely small and can be neglected. Therefore the transition energy is shared between the gamma ray and the lattice vibrations. A Mössbauer transition occurs if the state of the lattice remains unchanged, and the gamma ray gets the entire transition energy.

How is it possible that transitions can occur in which the lattice remains in its initial state? To obtain the answer, first the Einstein solid, and then the Debye solid will be considered.

The Einstein solid is a system of harmonic oscillators at one frequency.

The crystal vibrations are quantized and cannot receive an arbitrarily small amount of excitation energy. Since the Einstein solid has only one frequency, only one energy can be given to the solid:

$$E_E = \hbar\omega_E = k\Theta_E \qquad (2\text{-}1)$$

If the recoil energy R of the free nucleus is small compared to this excitation energy, the probability of emission of a phonon will be small, the lattice will not be excited, and the gamma ray will escape with the full transition energy.

The Debye solid is a system of harmonic oscillators with a spectrum of frequencies. The highest energy latttice vibration possible is given by

$$E_D = \hbar\omega_D \qquad (2\text{-}2)$$

where ω_D is the Debye cut-off frequency. This highest frequency vibration corresponds to the shortest possible wavelength $\lambda \approx 2d$, where d is the lattice constant. Thus the energy can be written

$$E_D = \hbar\omega_D = \hbar u \frac{2\pi}{\lambda} = 2\pi \frac{\hbar u}{2d} \qquad (2\text{-}3)$$

where u is the sound velocity in the solid.

In the Debye solid, lattice vibrations of frequencies lower than ω_D and wavelength longer than $\lambda \approx 2d$ are also possible.

These vibrations would require less energy than E_D. Thus, even though the recoil energy R may be less than E_D, it seems at first that R could be absorbed, resulting in no Mössbauer effect.

That these modes with smaller energy cannot be excited too easily may be seen by considering the following mechanical analogue.

Consider a system of a number of spheres which hang from a frame and touch each other. Lifting the outermost sphere, and letting it bump into the row excites a wave which travels through the chain and causes one sphere at the other end to jump off. In order to excite longer waves in this mechanical model, one lifts N spheres at one end, releases them, and N will bounce off at the other end.

Now consider the Debye solid again. The highest energy mode (i.e., with the shortest wavelength) corresponds to the situation where two adjacent atoms move out of phase. Such a wave can be excited most efficiently if the decaying atom is assumed to be free, receives its full share R of the recoil energy, and then bumps into a neighboring atom.

The lower energy modes have the longer wavelengths. A longer wave can be excited most efficiently in the solid if initially N atoms move together. Then the wavelength $\lambda \simeq 2Nd$ and the energy of this wave is

$$E = \hbar u \frac{2\pi}{2Nd} = \frac{E_D}{N} \qquad (2\text{-}4)$$

However, to excite this longer wave most efficiently, the N atoms must move together at the beginning, and the recoil energy must be transferred to these N atoms simultaneously. The decaying sytem is no longer one atom alone, but the N atoms together. The mass of the system is now NM where M is the mass of one atom. Therefore the recoil energy given to the system is

$$R_N = \frac{E_\gamma^2}{2NMc^2} = \frac{R}{N} \qquad (2\text{-}5)$$

The energy needed to excite this lower energy mode is E_D/N, however, only $R_N = R/N$ is available.

Therefore, if the recoil energy R of the free nucleus is small compared to the maximum excitation energy E_D, the probability of emission of a phonon will be small, the lattice will not be excited, and the gamma ray will escape with the full transition energy.

This treatment applies to the case when all the lattice oscillators are in their ground state (at 0^oK). At finite temperatures, some of the oscillators are excited and transitions with induced emission of phonons become possible.

Consideration of the physical picture of momentum conservation and energy conservation has thus shown that the Mössbauer effect is a physically possible phenomenon.

2.2 QUANTUM THEORY OF THE MÖSSBAUER EFFECT

In order to obtain an expression for the fraction of gamma rays emitted without energy loss to the lattice, a quantum mechanical treatment of the Mössbauer effect is needed.

At the same time this enables one to see what constitutes a good Mössbauer source. The initial part of this treatment follows closely that given by Frauenfelder [6], (p.26).

Initially, consider the case of emission or absorption of a gamma ray from a nucleus embedded in a solid with the lattice simultaneously changing state (a non-Mössbauer transition).

The probability of a transition in which the nucleus decays from the excited state N_i to the ground state N_f, while simultaneously the lattice goes from its initial state L_i to its final state L_f, is

$$W(N_i \rightarrow N_f, L_i \rightarrow L_f) = \text{constant} \left| \langle f | H_{int} | i \rangle \right|^2 \quad (2\text{-}6)$$

where $|i\rangle$ and $\langle f|$ denote the initial and final state of the entire system, and H_{int} is the interaction Hamiltonian responsible for this decay.

The energy that can be transferred to the lattice during this transition is very small compared to the gamma ray energy. Therefore the dependence of the density of final states $\varrho(E)$ on the energy transfer to the lattice is very small, and $\varrho(E)$ is assumed constant, being included in the constant of equation (2-6).

The Hamiltonian of a charged particle, moving with a momentum $\vec{p}$ in an electromagnetic field given by a vector potential $\vec{A}$, contains the term $\left[\vec{p} - \frac{e}{c}\vec{A} \right]^2$ This term leads to the nonrelativistic interaction Hamiltonian $H_{int} = B(\vec{p}\cdot\vec{A} - \vec{A}\cdot\vec{p})$, where B is a constant.

After expanding A in plane waves one obtains [7]

$$\langle f|H_{int}|i\rangle = B\langle f|\exp(i\vec{k}\cdot\vec{x})p_A|i\rangle \qquad (2\text{-}7)$$

where the gradient operator p_A must be applied in the direction of the polarization vector of the electromagnetic wave $\vec{k}$, and where $\vec{x}$ is the coordinate vector of the decaying nucleon. Thus, equation (2-7) corresponds to a single-particle description of the nucleus.

Lamb [5] states that because of the short range of the nuclear forces (and hence the independence of the motion in the crystal of the center of momentum and the internal degrees of freedom of the nucleus) the approximation that the nuclear decay is not influenced by the state of the lattice and that the lattice condition does not depend on the nuclear state, can be made. The state functions $|i\rangle$ and $\langle f|$ can then be written as products $|N_i\rangle\ |L_i\rangle$ and $\langle L_f|\langle N_f|$ of nuclear-state functions $|N_i\rangle$ and $\langle N_f|$ and lattice-state functions $|L_i\rangle$ and $\langle L_f|$, with $\langle L_f|L_i\rangle = \delta_{fi}$ and $\langle N_f|N_i\rangle = \delta_{fi}$.

Introduce internal nuclear coordinates $\vec{\varrho}$ by writing

$$\vec{x} = \vec{X} + \vec{\varrho} \qquad (2\text{-}8)$$

where $\vec{X}$ is the coordinate vector from the center of momentum of the entire crystal to the center of mememtum of the decaying nucleus, and where $\vec{x}$ is the coordinate vector from the center of momentum of the entire crystal to the radiating nucleon, while $\vec{\varrho}$ is the coordinate vector between the center of momentum of the decaying nucleus and the radiating nucleon.

The momentum operator also splits up into a sum

$$p_A = p_X + p_\rho \qquad (2\text{-}9)$$

where p_ρ acts on the internal nuclear coordinates and p_X on the center of momentum coordinates of the nucleus.

The matrix element of equation (2-7) can be separated into two parts, each consisting of a product of a nuclear and lattice matrix element by substituting (2-8) and (2-9) into it.

$$\langle f|H_{int}|i\rangle = B\left[\langle N_f|e^{i\vec{k}\cdot\vec{\rho}}p_\rho|N_i\rangle\langle L_f|e^{i\vec{k}\cdot\vec{X}}|L_i\rangle + \langle N_f|e^{i\vec{k}\cdot\vec{\rho}}|N_i\rangle\langle L_f|e^{i\vec{k}\cdot\vec{X}}p_X|L_i\rangle\right] \qquad (2\text{-}10)$$

To reduce (2-10) to a simpler form, consider the relative magnitudes of its two terms.

The closure[7] gives

$$\sum_{n'}|n'\rangle\langle n'| = 1 \qquad (2\text{-}11)$$

where the summation extends over all intermediate states.

Then the ratio of the lattice matrix elements in the two terms of (2-10) can be written

$$r_L = \frac{\langle L_f|e^{i\vec{k}\cdot\vec{X}}p_x|L_i\rangle}{\langle L_f|e^{i\vec{k}\cdot\vec{X}}|L_i\rangle} = \frac{\sum_{L'}\langle L_f|e^{i\vec{k}\cdot\vec{X}}|L'\rangle\langle L'|p_x|L_i\rangle}{\langle L_f|e^{i\vec{k}\cdot\vec{X}}|L_i\rangle} \qquad (2\text{-}12)$$

The momentum $\hbar\vec{k}$ transferred to the lattice during the nuclear decay is much larger than typical momenta components in the lattice. Therefore, the terms $\langle L_f|\exp(i\vec{k}\cdot\vec{X})|L'\rangle$ for allowed intermediate states L' are of the same order of magnitude as the term $\langle L_f|\exp(i\vec{k}\cdot\vec{X})|L_i\rangle$. Then they can be taken out from under the sum sign, giving

$$r_L \approx \sum_{L'}\langle L'|p_x|L_i\rangle = \langle p_L\rangle \qquad (2\text{-}13)$$

where $\langle p_L \rangle$ denotes an average over lattice momentum components.

Similarily, the ratio of nuclear matrix elements is

$$r_N = \frac{\langle N_f | e^{i\vec{k}\cdot\vec{\rho}} p_\rho | N_i \rangle}{\langle N_f | e^{i\vec{k}\cdot\vec{\rho}} | N_i \rangle} = \frac{\sum_{N'} \langle N_f | e^{i\vec{k}\cdot\vec{\rho}} | N' \rangle \langle N' | p_\rho | N_i \rangle}{\langle N_f | e^{i\vec{k}\cdot\vec{\rho}} | N_i \rangle} \qquad (2\text{-}14)$$

The momentum transfer $\hbar\vec{k}$ is much smaller than typical nuclear momentum components. Thus the ratio of the nuclear matrix elements (2-10) is

$$r_N = \sum_{N'} \langle N' | p_\rho | N_i \rangle = \langle p_N \rangle \qquad (2\text{-}15)$$

Therefore, since $\langle p_N \rangle$ is much greater than $\langle p_L \rangle$, the second term in equation (2-10) can be neglected, and (2-10) reduces to

$$\langle f | H_{int} | i \rangle = \langle L_f | e^{i\vec{k}\cdot\vec{X}} | L_i \rangle \langle N \rangle \qquad (2\text{-}16)$$

Calculation of the fraction f of gamma rays emitted without energy loss to the lattice ($L_i \rightarrow L_i$) can now be made from (2-16).

$$f = \frac{|\langle L_i | e^{i\vec{k}\cdot\vec{X}} | L_i \rangle|^2}{\sum_{L_f} |\langle L_f | e^{i\vec{k}\cdot\vec{X}} | L_i \rangle|^2} \qquad (2\text{-}17)$$

By using equation (2-11) again

$$\sum_{L_f} |\langle L_f | e^{i\vec{k}\cdot\vec{X}} | L_i \rangle|^2 = \sum_{L_f} \langle L_i | e^{-i\vec{k}\cdot\vec{X}} | L_f \rangle \langle L_f | e^{i\vec{k}\cdot\vec{X}} | L_i \rangle$$

$$= \langle L_i | e^{-i\vec{k}\cdot\vec{X}} e^{i\vec{k}\cdot\vec{X}} | L_i \rangle = 1$$

Therefore the fraction of Mössbauer gamma rays is given by

$$f = |\langle L_i | e^{i\vec{k}\cdot\vec{X}} | L_i \rangle|^2 \qquad (2\text{-}18)$$

This fraction f is often called the Lamb-Mössbauer factor, and is analogous to the Debye-Waller factor used for the scattering of x-rays without loss of energy to the lattice.

In order that the probability of the Mössbauer effect can be related to the Einstein solid and the Debye solid, normal lattice coordinates must be introduced. Lipkin's[8] method will be used. Assume that the interatomic forces are harmonic so that a simple transformation to normal modes is possible. These modes will be described by normal coordinates q_s. The state of the lattice can be specified by the set of quantum numbers (n_s) describing the state of excitation of each normal mode.

Then
$$\vec{\varepsilon}_k \cdot \vec{X} = \sum_s a_s q_s \qquad (2\text{-}19)$$
where $\vec{\varepsilon}_k$ is a unit vector in the direction of the vector $\vec{k}$.

Substituting equation (2-19) into equation (2-18) gives

$$f = |\langle (n_s)| e^{ik\sum_s a_s q_s} |(n_s)\rangle|^2 = \prod_s |\langle n_s| e^{ik a_s q_s} |n_s\rangle|^2 \qquad (2\text{-}20)$$

Lipkin's method of evaluating equation (2-20) gives

$$f \approx \exp \sum_s \left[-k^2 a_s^2 \langle n_s | q_s^2 | n_s \rangle \right] \qquad (2\text{-}21)$$

The expectation value of q_s^2 in the state n_s is evaluated by noting that the potential energy for a harmonic oscillator $\frac{1}{2} M\omega_s^2 q_s^2$, has an expectation value of $(n_s+\frac{1}{2})\hbar\omega_s/2$, where ω_s is the oscillator frequency for the s mode.

Therefore

$$f \approx \exp \sum_s \left[-(2n_s+1) \frac{(\hbar k)^2}{2M} \frac{a_s^2}{\hbar\omega_s} \right] \qquad (2\text{-}22)$$

The factor $(\hbar k)^2/2M\hbar\omega_s$ is the ratio of the free recoil energy to the energy of the s^{th} lattice vibration normal mode. If the lattice is in its lowest state (at 0°K), every n_s is zero and the exponent in (2-22) becomes the ratio of the free recoil energy to some average lattice vibration energy $\hbar\omega_{AV}$ defined by

$$\frac{1}{\hbar\omega_{AV}} = \sum_s \frac{a_s^2}{\hbar\omega_s} \qquad (2\text{-}23)$$

At absolute zero then, equation (2-22) reduces to

$$f = e^{-\frac{R}{\hbar\omega_{AV}}} \qquad (2\text{-}24)$$

where $R = \frac{(\hbar k)^2}{2M}$ is the free recoil energy.

From equation (2-24) it can be seen that the probability of an effect decreases very rapidly if the free recoil energy increases above this average lattice energy.

For the Einstein solid

$$\hbar\omega_{AV} = \hbar\omega_E = k\Theta_E$$

which, when substituted into equation (2-24), gives

$$f = e^{-\frac{R}{k\Theta_E}} \qquad (2\text{-}25)$$

For the Debye solid

$$\hbar\omega_{AV} = \tfrac{2}{3}\hbar\omega_{MAX} = \tfrac{2}{3}k\Theta_D$$

which, when substituted into equation (2-24), gives

$$f = e^{-\frac{3}{2}\frac{R}{k\Theta_D}} \qquad (2\text{-}26)$$

From equations (2-22), (2-25) and (2-26), the conditions which increase or decrease the probability of the Mössbauer effect can be seen.

The temperature dependence of the Mössbauer effect can be seen in the term $(2n_s+1)$ of equation (2-22), and

understood as stimulated emission and absorption of phonons, since the probability of energy exchange between the lattice and the recoiling nucleus increases with the degree of excitation of the lattice.

From (2-25) or (2-26), it can be seen that the recoil energy R should be small, with the resulting requirement that the gamma ray energy should be small. These two equations also show that the Einstein temperature or the Debye temperature of the solid should be high. Care must be taken, however, since the average lattice vibration energy (equation 2-23) does not involve the same kind of average used to compute such properties as specific heats. Only for simple models is there a simple relation between the average lattice vibration energy and the Debye temperature. These two temperatures will, however, have the same order of magnitude.

The exponential dependence in equations (2-22), (2-25) and (2-26) shows that a small change in their parameters can have a large effect on the experiment. Therefore, in calculating the probability of the effect, an incorrect interpretation of the Debye temperature would give a wrong result. Also, in actually carrying out the experiment, a constant ambient temperature is important.

In summary, a good Mössbauer source is one with a low energy gamma ray, and thus a low free recoil energy R, a high "Debye-Mössbauer" characteristic temperature, and located in a low temperature environment.

2.3 LIFETIME OF THE EXCITED STATE

The resonance curve of the Mössbauer effect obtained by measuring the transmission of the gamma rays has been found to have a line-width of 2Γ (see Figure 1-3). The natural line-width and the lifetime of the excited state are related by Heisenberg's uncertainty principle;

$$\tau \cdot \Gamma = \hbar \qquad (2\text{-}27)$$

Therefore, by measuring the line-width of the resonance curve, a measure of the lifetime can be obtained.

However, various effects can broaden the line, resulting in an apparent lifetime shorter than the actual lifetime. Electronic measurements can give a more accurate measure of the lifetime, but the Mössbauer effect does at least give an easy indication of it.

The measured line-width is made up of a number of contributions. Basically, there is the natural line-width of the absorber and the natural line-width of the source. In addition, there is the broadening due to finite thickness of the absorber and also finite velocity resolution of the apparatus. However, the main influences which could broaden the line-width beyond 2Γ are the extra-nuclear effects. The line-width is strongly dependent on the compositions of the source and absorber. For example, Fe^{57} nuclei in natural iron exhibit hyperfine splitting, whereas Fe^{57} nuclei in copper exhibit a line-width fairly close to the natural line-width. A slight magnetic broadening could occur if the electron spin correlation time (sec. 2.5) was not quite

sufficiently short to destroy all hyperfine interaction. Quadrupolar broadening could arise because of interactions between the quadrupole moment and the electric field gradients produced by the spatial charge density fluctuations around an impurity atom. Inhomogeneous broadening may arise because of the variation of environments experienced by the various source (or absorber) atoms in the alloy, which could result in shifting of the nuclear energy levels.

As a result of these many broadening effects which may act on the natural line-width, experimental line-widths are generally considerably wider than the line-widths calculated from electronically obtained lifetimes. The Mössbauer effect does, however, give a lower bound to the lifetime of the excited state.

2.4 ISOMER SHIFT THEORY

Ideally, the Mössbauer resonance curve should show maximum resonance absorption at zero velocity. However, certain perturbations cause the curve center to be shifted away from zero velocity. For this reason, results from positive and negative velocities of the source or absorber are not added together, but kept separate.

There are two main shifts, the second-order Doppler shift [9] and the nuclear isomer shift. [10] The former is much smaller than the latter.

Consider the second-order Doppler shift first. When the excited state decays by gamma-ray emission, the nucleus

loses energy, and its mass is changed by an amount $\Delta M = -\frac{E}{c^2}$. Its thermal momentum p is unchanged, since the solid takes up all the recoil momentum. However, the reduced mass causes an increase in the kinetic energy of the emitting nucleus;

$$\Delta E_{kin} = \left(\frac{\Delta E_{kin}}{\Delta M}\right)\Delta M = \left(\frac{-p^2}{2M^2}\right)\left(\frac{-E}{c^2}\right) = \frac{1}{2} E \frac{\overline{v^2}}{c^2} \qquad (2\text{-}28)$$

where $\overline{v^2}$ is the mean square velocity of the emitting nucleus. As a consequence, the energy of the emitted gamma ray is decreased by the same amount. A corresponding shift occurs during the absorption process, so that any experiment measures only the difference $\overline{v_s^2} - \overline{v_a^2}$. If the environments of the source and absorber nuclei are the same, the shifts will be the same since the velocities will be equal, and no shift will be experimentally observable. However, if the source and absorber are at different temperatures, or if the source and absorber nuclei are in different surroundings, a shift can result. The magnitude of the shift is very small.

The isomer shift arises from the electrostatic interaction between the nuclear charge distribution and the electronic charge density at the nucleus. The s-electrons are involved since only they have a finite probability density at the origin. The binding energy of an s-electron is reduced in proportion to the volume occupied by the nuclear charge when compared with the value corresponding to a point nucleus. The ground and isomeric levels of the nucleus have different effective charge radii. Therefore, the electrostatic interaction with the electronic charge is different in the

two states. The gamma ray energy is consequently changed (relative to its value for a point nucleus) by an amount proportional to the s-electron density at the nucleus. If the s-electron density is different for the source and the absorber, the difference in isomer shift between the two can be obtained experimentally. If the source and absorber atoms are embedded in identical compounds, their nuclear levels will be shifted equal amounts, and no isomer shift will be observed.

The measured isomer shift difference will be proportional to the difference in nuclear charge radii between the ground and excited states, and also to the difference in the s-electron densities between the two compounds hosting the source and absorber atoms.

For an example, consider the case of the nuclear charge radius greater in the ground state, and the s-electron density greater in the absorber.

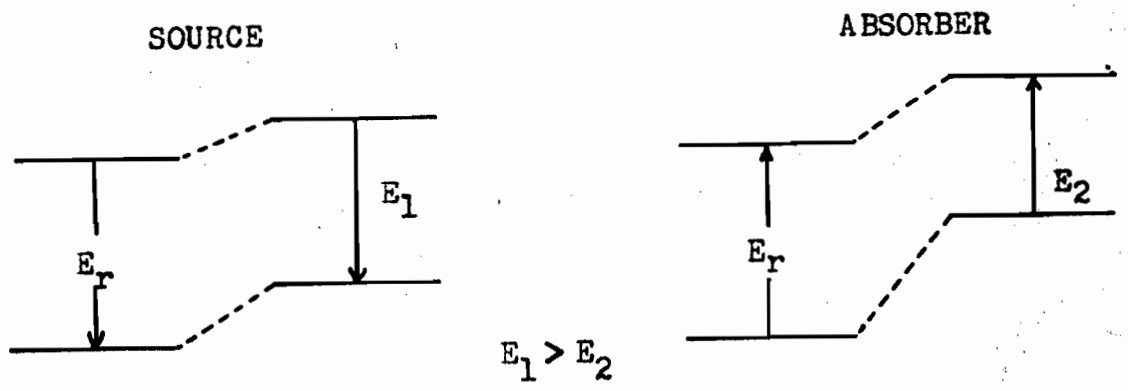

FIGURE 2-1 ORIGIN OF THE ISOMER SHIFT

In each case, the energy levels on the left are appropriate to a point nucleus, and those on the right indicate the change introduced by the finite charge distribution. In this case $E_1 > E_2$, so that the source energy needs to be decreased to produce exact resonance. The whole curve would be shifted from zero velocity, showing the difference in isomer shift.

By examining the isomer shift in a large number of chemical compounds it is possible to identify fully ionic compounds of different valency. For these ions, the difference in the s-electron density can be calculated, so that the isomer shift can give the change in charge radius.

In the absence of phase changes, the value of the s-electron density should not change appreciably with temperature, so that the isomer shift may usually be regarded as temperature independent. This makes it possible to separate the contributions of the isomer shift, and the temperature dependent second order Doppler shift. If the source and absorber are at the same temperature, the second order Doppler shift is considered negligible compared to the isomer shift.

2.5 INTERNAL FIELD THEORY

For determination of the lifetime of the excited state of a Mössbauer source, the emission and absorption lines are unsplit, each having approximately the natural line-width, however, there are cases for which both emission and absorption spectra are split into a number of components. The nuclear energy levels can be split by the interaction

between the nuclear magnetic moment and the internal field. By putting the source and absorber atoms in appropriate host lattices, the Mössbauer effect can thus be used to determine the hyperfine splittings of the ground and excited states, the magnitude of the internal field at the nucleus and the nuclear magnetic moment of the excited state.

The magnetic moment of the nucleus can interact with an externally applied field or with unpaired electrons of the atom and its neighbours. The magnetic interaction with electrons is of two types [11]. For s-electrons it is a contact interaction proportional to the spin density at the nucleus for the unpaired electrons, and for other electrons it is a dipole-dipole interaction. Thus, the internal field represents the magnetic interaction of the surrounding electrons with the nucleus. The Hamiltonian describing the coupling of the nuclear magnetic moment with the internal magnetic field is

$$\mathcal{H}_M = -g_I \vec{I} \cdot \vec{H} \qquad (2\text{-}29)$$

In the presence of this field, the spatial degeneracy of the nuclear spin $\vec{I}$ is removed and each nuclear level is split into its $(2I+1)$ components. The energy shift of the sub-state m_I is then

$$\Delta E = -m_I g_I H \qquad (2\text{-}30)$$

where g_I is the nuclear gyromagnetic ratio μ_I/I.

Consider the case of a ferromagnetic material. In a ferromagnetic material, the exchange energy is relatively large and therefore the electron spins will be aligned. The

nucleus then sees a strong constant magnetic field, with very little fluctuating component. As a result, hyperfine splitting is observed.

For the case of a paramagnetic material, the electron spins are not aligned. An internal field exists from the unpaired electrons, but a corresponding splitting of the nuclear energy levels is not observed. If the spin correlation time, which is the time during which the electron spin points in a definite direction, is small compared to the period of the nuclear Larmor precession frequency in the internal field, only an average internal field will be seen by the nucleus, and this is zero unless the paramagnetic ion is in a magnetically ordered lattice.

The Mössbauer source to be used here, Fe^{57}, is itself ferromagnetic. Thus, Fe^{57} in iron will result in hyperfine splitting. In order to obtain an unsplit source or absorber an alloy or compound of Fe^{57} that is paramagnetic (or diamagnetic) is required. By putting a small enough concentration of Fe^{57} into a paramagnetic material, the iron spins will not be aligned, the time average field at the iron nucleus will be zero, and an unsplit energy results.

The most common method of obtaining an unsplit source is putting Fe^{57} in 310 stainless steel (25% chromium, 20% nickel) which is paramagnetic. The process consists of evaporating $Co^{57}Cl_2$ solution to dryness on stainless steel and diffusing at 950^{o} C in an evacuated quartz capsule.

Another host lattice often used is copper, which is also paramagnetic. This process consists of electroplating Co^{57} onto a copper foil, followed by diffusion by annealing.

To observe the hyperfine splitting, an unsplit source and split absorber combination will give the simplest resonance pattern. When both source and absorber are split, the pattern can be very complicated, for overlap of any emission line with any absorption line gives resonance absorption.

CHAPTER III

APPARATUS

3.1 GENERAL CONSIDERATIONS.

Nearly all work on the Mössbauer effect is done by observing the transmission of the gamma rays. The main reasons for using transmission instead of scattering are the relatively large effects, the large intensities and favorable geometry obtainable in transmission. The intensity, which is already low in a scattering experiment, is further decreased by the strong conversion of low energy gamma rays; only a fraction $1/(1+\alpha)$ of the absorbed gamma rays is reemitted (where α is the internal conversion coefficient). However, when the Mössbauer effect is very small or when it is reduced by the presence of non-resonant radiation of nearly the same energy which cannot be eliminated by either critical absorbers or high resolution of the detector, it may be more efficient to perform the experiment with a scattering geometry. Various scattering experiments have been carried out by Barloutaud [12], Frauenfelder[13], Kankeleit[14], and Mitrofanov [15]. The work reported here was done with a transmission geometry.

There are two main ways of obtaining the resonance pattern. In one, the source (or absorber) is moved at a constant velocity for a pre-set time and the counts during this period are recorded. The velocity is then changed to a new value and the procedure is repeated until the entire pattern is obtained. This is the method used here.

In the second method, the source sweeps periodically through a range of velocities and the counts in predetermined velocity intervals are stored in different channels of a multichannel analyzer. This method gives a first impression of the entire resonance pattern very quickly. The advantage of the constant velocity method is that any specific part of the pattern can be investigated in great detail. Both methods, however, gather information at the same rate.

The constant velocity method is liable to inaccuracy if there are any drifts in the counting circuits. Since change in counting rate is the way the Mössbauer effect is detected, any drift could have a serious effect on the resonance pattern. If the method is used over a long period of time, corrections for decay of the source must be made. In addition, experimentally, it is generally desirable to see the entire pattern as quickly as possible. For these reasons the velocity sweep method would be preferable. It involves considerably more equipment however, and for this reason, these initial Mössbauer experiments were done by the constant velocity method.

Table 3-1 gives the important component instruments used here. Figure 3-1 gives a picture of the entire apparatus as built and used, and Figure 3-3 is a block diagram showing the functions of the various components.

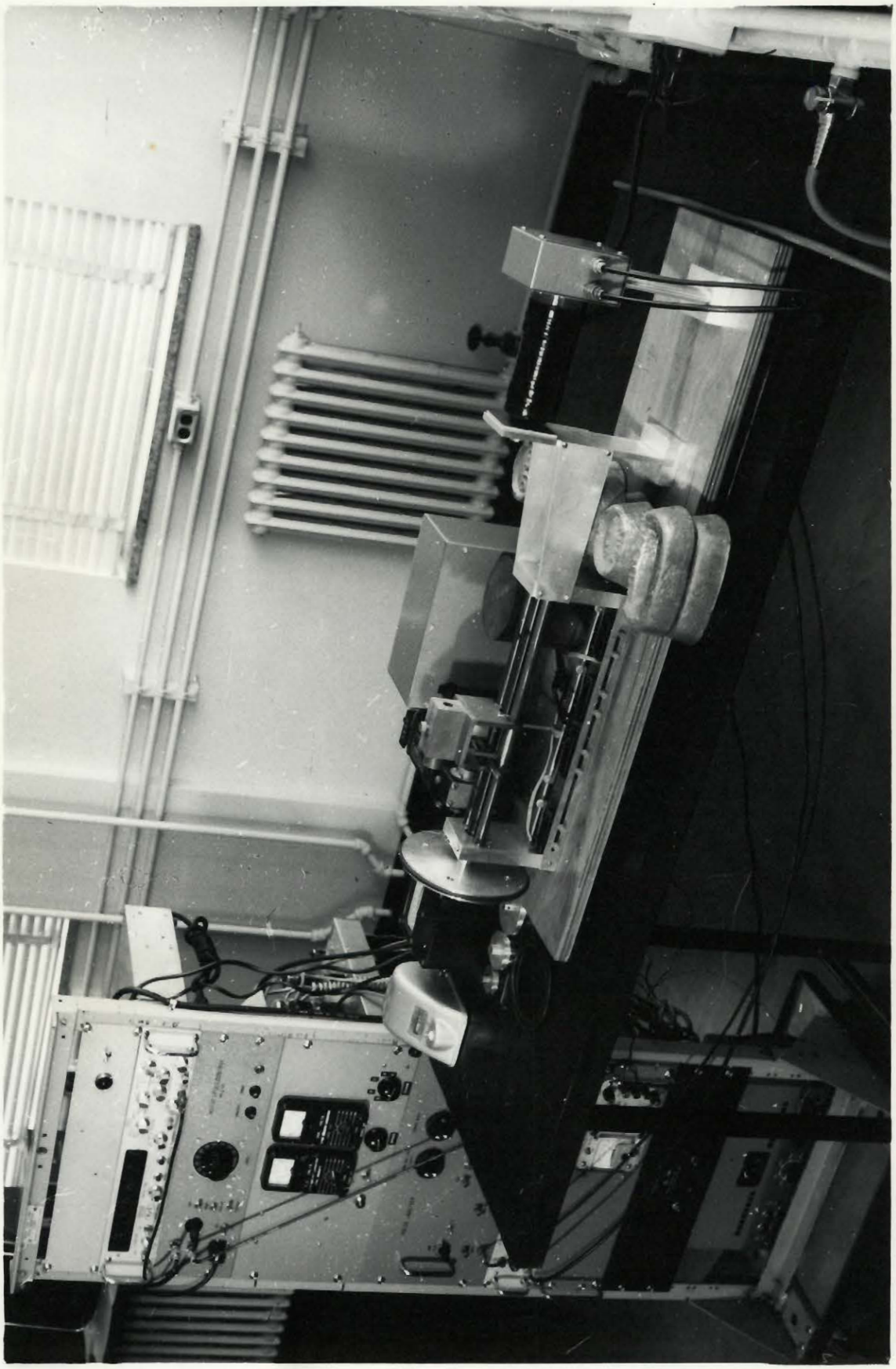

FIGURE 3-1 THE MÖSSBAUER EFFECT APPARATUS

3.2 THE MÖSSBAUER SOURCES

A considerable number of transitions which exhibit the Mössbauer effect have been discovered and tabulated.[11] There remains, however, one transition which has been used most extensively: the 14.37 kev gamma ray of Fe^{57}. The 14.37 kev level is an excited state with a mean lifetime of 1.4×10^{-7} sec, resulting in a very narrow natural line-width of 4.7×10^{-7} ev. As a result of the low gamma ray energy involved, and the high Debye temperature of Fe, a very strong resonance is obtainable even at room temperature.

The radioactive Fe^{57} is obtained by the decay by K-electron capture and neutrino emission of the ground state of Co^{57}, which has a half-life of 270 days [16]. It decays to a second excited state of Fe^{57} which has a mean lifetime of about 9×10^{-9} sec. This state decays by emission of a 123 kev gamma ray to the first excited state of Fe^{57}. A minor fraction (9%) of the decays of the second excited state involve a transition directly to the ground state by emission of a 137 kev gamma ray. The transition of the first excited state to the ground state by emission of a 14.37 kev gamma ray is the Mössbauer transition.

As discussed in section (2.5), Fe^{57} is ferromagnetic, and when placed in an Fe lattice, the emission spectrum exhibits hyperfine splitting. In order to determine the effects of different host lattices on the hyperfine splitting and the internal field, the following host lattices with Co^{57} were used as sources:

1. Copper 0.0025 inch thick
2. 310 stainless steel 0.001 inch thick
3. iron 0.00035 inch thick

Each of these sources had an activity of 2 millicuries.

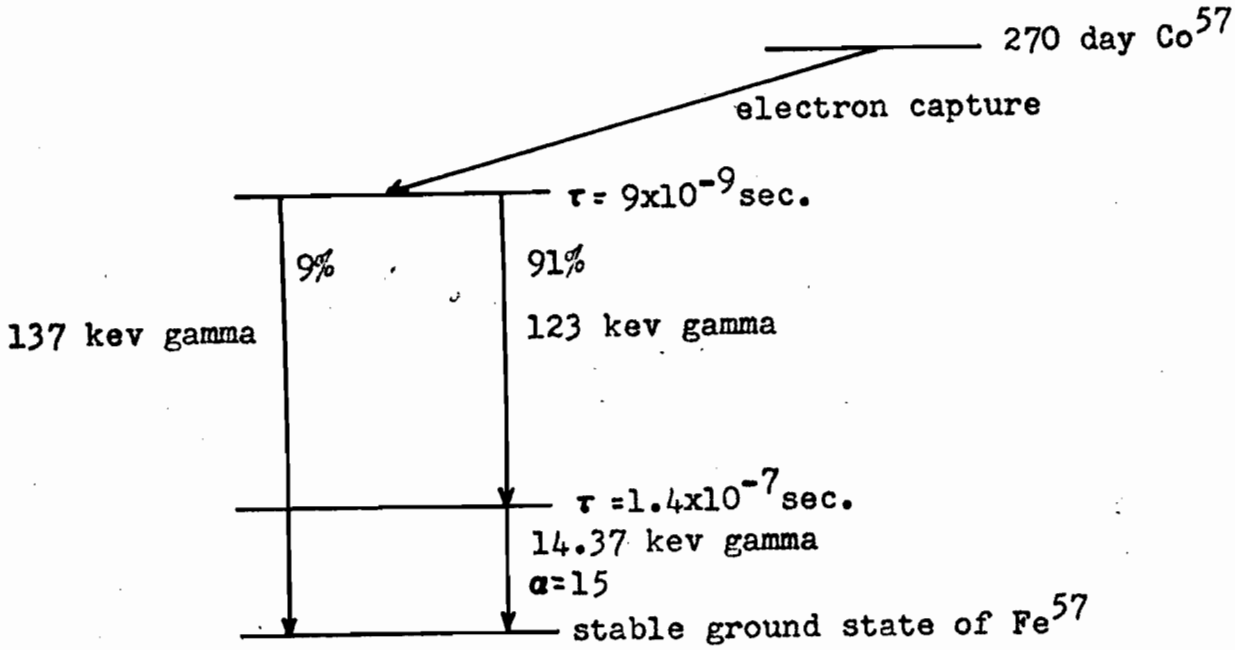

FIGURE 3-2 DECAY SCHEME OF Fe^{57}

3.3. THE ABSORBERS

One of the basic requirements for resonance absorption is the presence in the absorber of atoms of the stable isotope. In the case of Fe^{57}, there are a number of advantages to using as an absorber a substance which is naturally iron-bearing. One is that the iron is in a normal lattice site, rather than in a site characteristic of cobalt. Another is that there is no preceding electron-capture decay, which could result in a displaced or multiply ionized atom. The concentration of iron in the material should be high enough so that an absorber of areal density 0.1 mg/cm^2 of Fe^{57} can be made.[17] Since the natural abundance of Fe^{57} is only 2.14%, the use of the enriched isotope may be desirable. The absorber should not be thick since when a Doppler shift measurement is made, selective absorption occurs and the line appears broadened.

In conjunction with the investigations of the internal field mentioned in section (3.2), the following host lattices with Fe^{57} were used as absorbers:

1. 310 stainless steel 0.001 inch thick
2. 310 stainless steel 0.00015 inch thick
3. natural iron 0.001 inch thick
4. enriched Fe^{57} 91.1%, 1.9 mg/cm^2, 0.0001 inch thick.

These were used in various combinations with the sources listed in section (3.2).

3.4 THE VELOCITY DRIVE

The resonance pattern of the Mössbauer effect is observed by Doppler shifting the gamma ray energy by giving the source and absorber definite relative velocities. This is usually done by moving the source or absorber (whichever is experimentally convenient) while the other is kept fixed.

The velocity drive used here moved the source, while the absorber was held stationary. The source was mounted on a carriage which was driven by a screw arrangement. The carriage path length was 22.50 cms. Microswitches at either end of the screw reversed the motion which provided by a $\frac{1}{10}$ hp d-c shunt motor. The motor speed was kept constant by a feedback control system which also enabled a fairly wide range of velocities to be obtained. In order that the velocity could be varied from 0.1 mm/sec to 11 mm/sec, a system of pulleys was used in conjunction with the feedback motor speed control.

A constant velocity and vibration-free drive is necessary for a Mössbauer experiment. For these reasons counting was not begun until the velocity had stabilized after motor reversal. This was accomplished by a pair of microswitches set 2.65 cms and 5.45 cms inside the reversing microswitches. This gave a usuable source path length of 14.40 cms. This counting gate served another purpose also. The counting rate which was detected by a scintillation counter at one end of the velocity drive was considerably higher at the end closest to the detector than at the end farthest from the

detector. Therefore, each velocity run was made over the same part of the source path length. Since the microswitches did not trip at the same carriage position when the motion was in opposite directions, when changing from taking results in the positive direction to taking results in the negative direction, both counting gate microswitches had to be adjusted to ensure counting over the same part of the path length. The positive direction is defined as that for which the source is moving toward the absorber.

The counting gate microswitches were connected to relay circuits which allowed counting in one direction only. Thus, the counter could collect counts from a number of runs, but they were only those for the desired direction. (Because of shifts such as the isomer shift, the counting rate in the positive direction does not necessarily equal that in the negative direction and the results from the two directions must be kept separate).

To determine the velocity accurately, a timer was also connected to the counting gate relay circuit. The timer measured the interval during which counts were being collected, and for one run, measured the length of time for the source to move between the counting gate microswitches. Thus by accurately knowing the distance between the microswitches and the length of time, the velocity was determined. Over a large number of runs the velocity was constant to within 0.1% to 0.8%. The timer was accurate to $\pm$ 0.02 seconds.

Vibrations in the velocity drive were considerably

damped by the use of rubber mounts, and by placing heavy weights on the velocity drive mounting board. Also, the screw arrangement and carriage path were designed and carefully machined to keep vibration to a minimum.

There are a number of different methods of Doppler shifting the gamma ray energy. Each method must be able to give a constant, definite velocity, free of vibration, to the source or absorber, and the counts and the time must be obtained from the same part of the path length on each run. Each method must also be able to separate the positive and negative direction results. The velocity drive used here fulfills these requirements.

3.5 THE DETECTION AND COUNTING APPARATUS

Detection of the Mössbauer effect depends upon observing a change in the counting rate as a function of velocity. As a result the detection and counting circuit must be stable.

The detector consisted of a NaI(Tl) crystal sealed to an RCA 6655-A photomultiplier tube. Scintillation pulses corresponding to energies in the neighborhood of 14 kev were counted by means of a Model 60 amplifier and single channel analyzer, and a TSI digital counter.

From time to time during the course of the experiments, a counting rate discontinuity was noted. The counting rate would drop sharply, and then return to its original rate. However, by recording the number of counts in each run, any such discontinuity could be noted. In addition, there was a slight drift in counting rate due to temperature sensitivity of the detector circuit. By continuous plotting of the results and by checking the counting rate at a previous point or at a point where all resonance absorption was destroyed, a constant check on any counting rate drift was kept. This counting rate instability shows the disadvantage of the constant velocity method of obtaining the resonance pattern. It takes a considerable length of time to obtain a complete pattern, and a slight counting rate drift may lead to inacccurate results. The velocity sweep method, on the other hand, presents the entire pattern almost immediately, and the effect of a slight drift would be lessened because it would be applied to the entire resonance pattern.

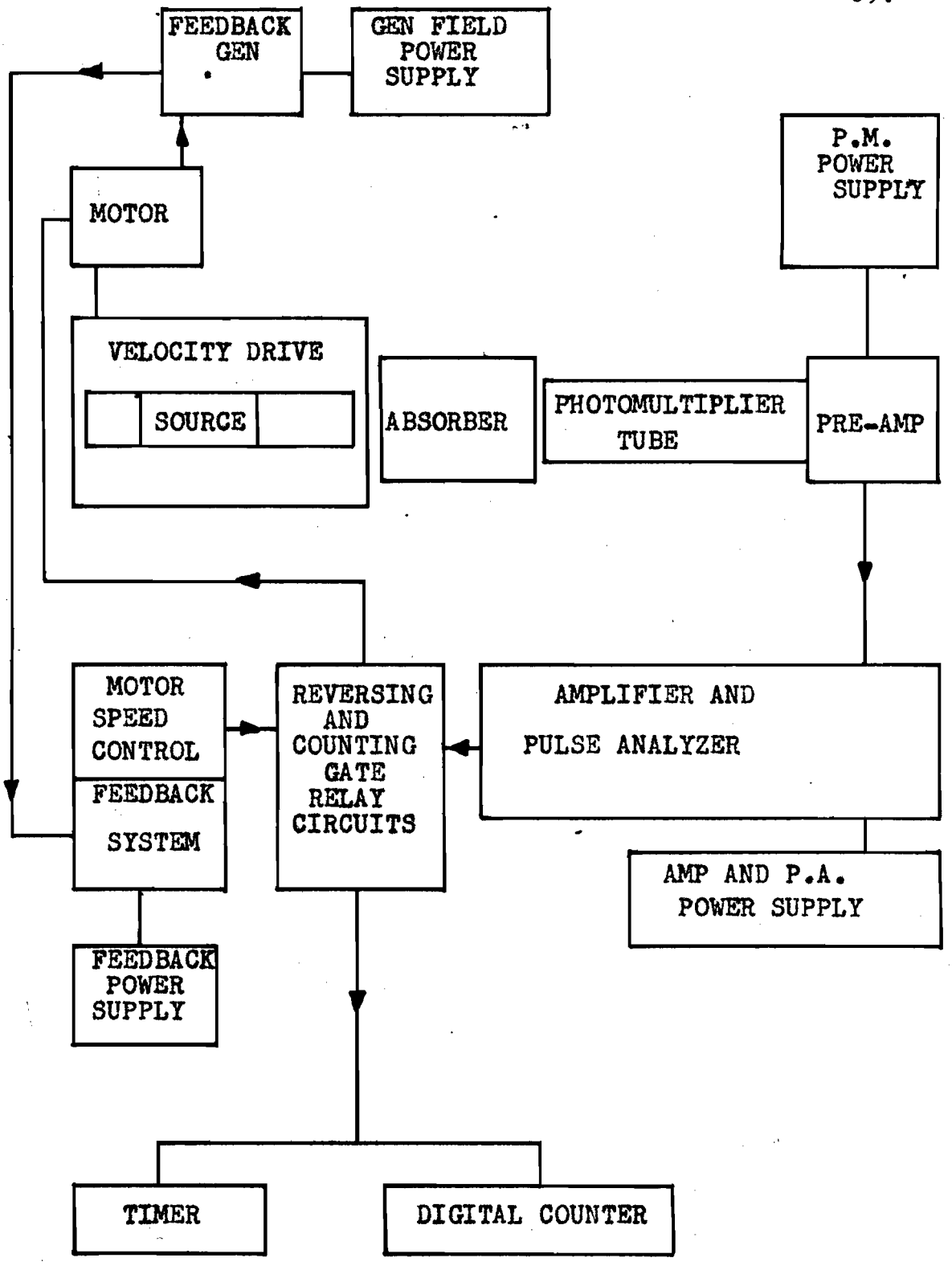

FIGURE 3-3 FUNCTIONAL BLOCK DIAGRAM

Table 3-1 IMPORTANT COMPONENT INSTRUMENTS

Sources and Absorbers	Nuclear Science and Engineering Co.	
Velocity Drive	Made in Shop	
Velocity Drive Motor	Small Electric Motors (Can.) Ltd.	7113-A
Motor Speed Control and Feedback System	Dyer and Smee	
Photomultiplier Tube	Electron Tube Division, R.C.A.	6655-A
Amplifier and Pulse Analyzer	Made in Shop from McGill Radiation Laboratory Circuit	60
Digital Counter	Transistor Specialties, Inc.	361R
Timer	Precision Scientific Co.	69230
Photomultiplier Power Supply	John Fluke Mfg. Co.,Inc.	412A
Amplifier and Pulse Analyzer Power Supply	Lambda Electronics, Corp.	28
Feedback Power Supply	Lambda Electronics, Corp.	25
Generator Field Power Supply	Power Designs Inc.	4005R

CHAPTER IV

THE RESULTS AND THEIR INTERPRETATION

4.1 THE Fe^{57} SPECTRUM

The Fe^{57} spectrum was studied in detail, mainly in order to determine the pulse analyzer settings, but also in order to obtain general information about it.

A considerable amount of noise was detected in the very low energy part of the spectrum (see Figure 4-1), but the 14.4 kev gamma was still resolved. The highest peak is the 123 kev gamma and the 137 kev gamma, both appearing as one peak. The lower peak to the left of the highest one is the iodine escape peak.

A thin NaI(Tl) scintillation counter was used to detect the 14.4 kev radiation. To obtain better resolution of this radiation against background, a gas-filled proportional counter should have been used.

The detailed spectrum of the 14.4 kev gamma, indicated that the center of the peak was at 10 volts with minima on either side at 6 volts and 17 volts. As a result, the main bias of the pulse analyzer was set at 6 volts, and the channel width at 10 volts. (Counts are then accepted between 6 and 16 volts.)

Movement of the 14.4 kev peak was checked on three consecutive days, and then at three other times during the experiment to ensure that the analyzer was still set for the Mössbauer transition.

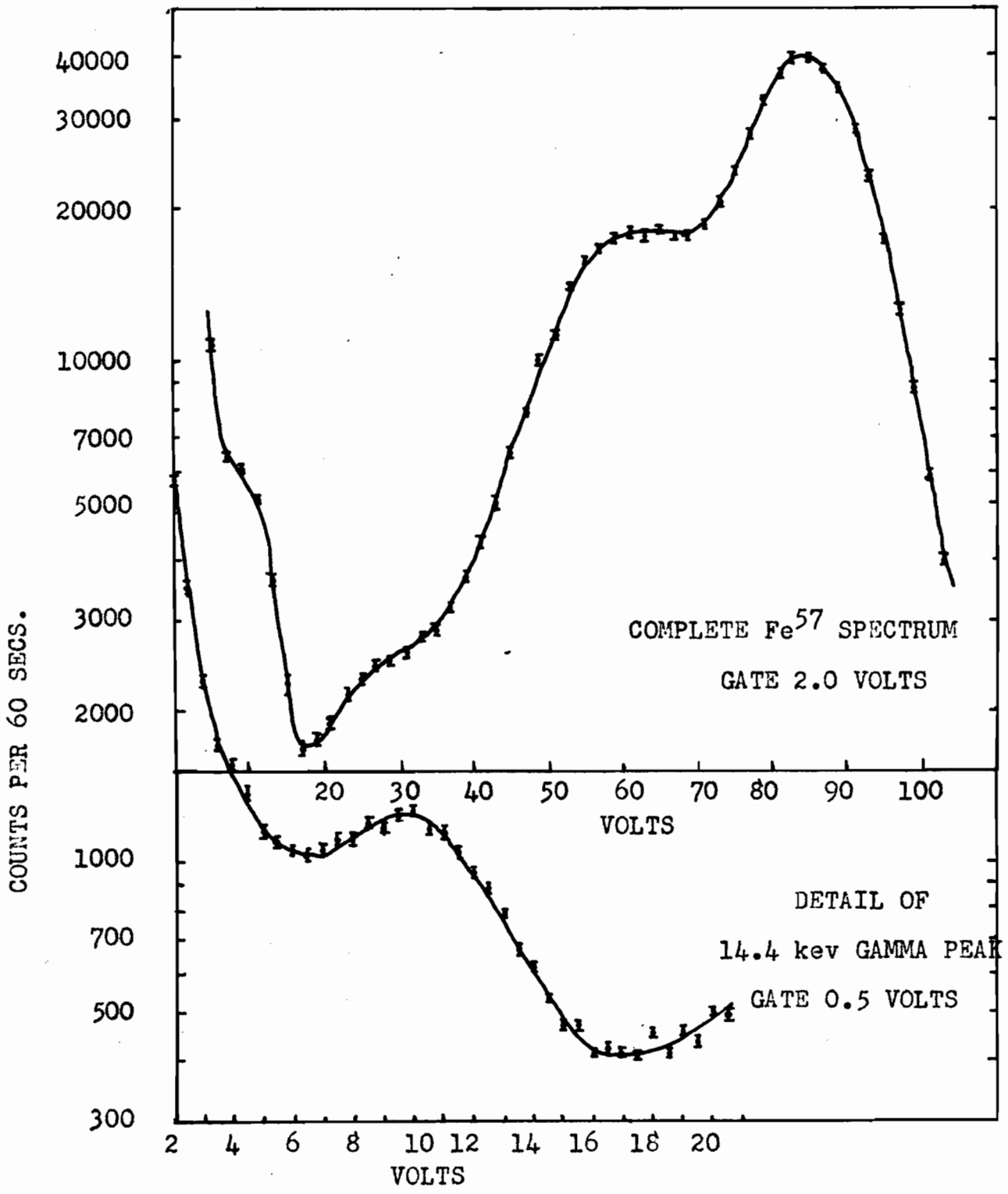

FIGURE 4-1 GAMMA RAY SPECTRUM OF Fe^{57}

4.2 THE UNSPLIT SPECTRA

Diffusing Fe^{57} into a suitably paramagnetic material results in an unsplit line. If both the source and absorber energies are unsplit, a single resonance curve is obtained. As discussed in sections (2.3) and (2.4), these unsplit spectra can be used to give values for the mean lifetime of the first excited state of Fe^{57} and the isomer shift.

4.21 Cu Source and 310 Stainless Steel Absorber 0.001 inch thick.

The line-width of this curve (see Figure 4-2) is (0.55 ± 0.05)mm/sec. To convert this velocity to energy units, the Doppler shift equation is used.

$$\Delta E = \frac{v}{c} E_r \qquad (4\text{-}1)$$

where ΔE is the resultant energy shift,

v is the velocity of the source

c is the velocity of light, taken to be 3.00×10^{11} mm/sec, and

E_r is the transition energy, in this case 14.37 kev.

Thus, using (4-1) the curve width is $(26.35\pm2.40)\times10^{-9}$ev. Theoretically this width is twice the natural line-width (see the chapterIdiscussion of Figure 1-3). Thus the actual line-width of this curve is $\Gamma = (13.18\pm1.20)\times10^{-9}$ev. Then, by using equation (2-27),

$$\tau \cdot \Gamma = \hbar \qquad (2\text{-}27)$$

the mean lifetime of the excited state can be calculated, where $\hbar = 6.58\times10^{-16}$ev is used.

Therefore, $\tau = (0.50\pm0.04)\times10^{-7}$secs. This compares with the electronic measurement of $\tau = 1.4\times10^{-7}$sec, indicating that

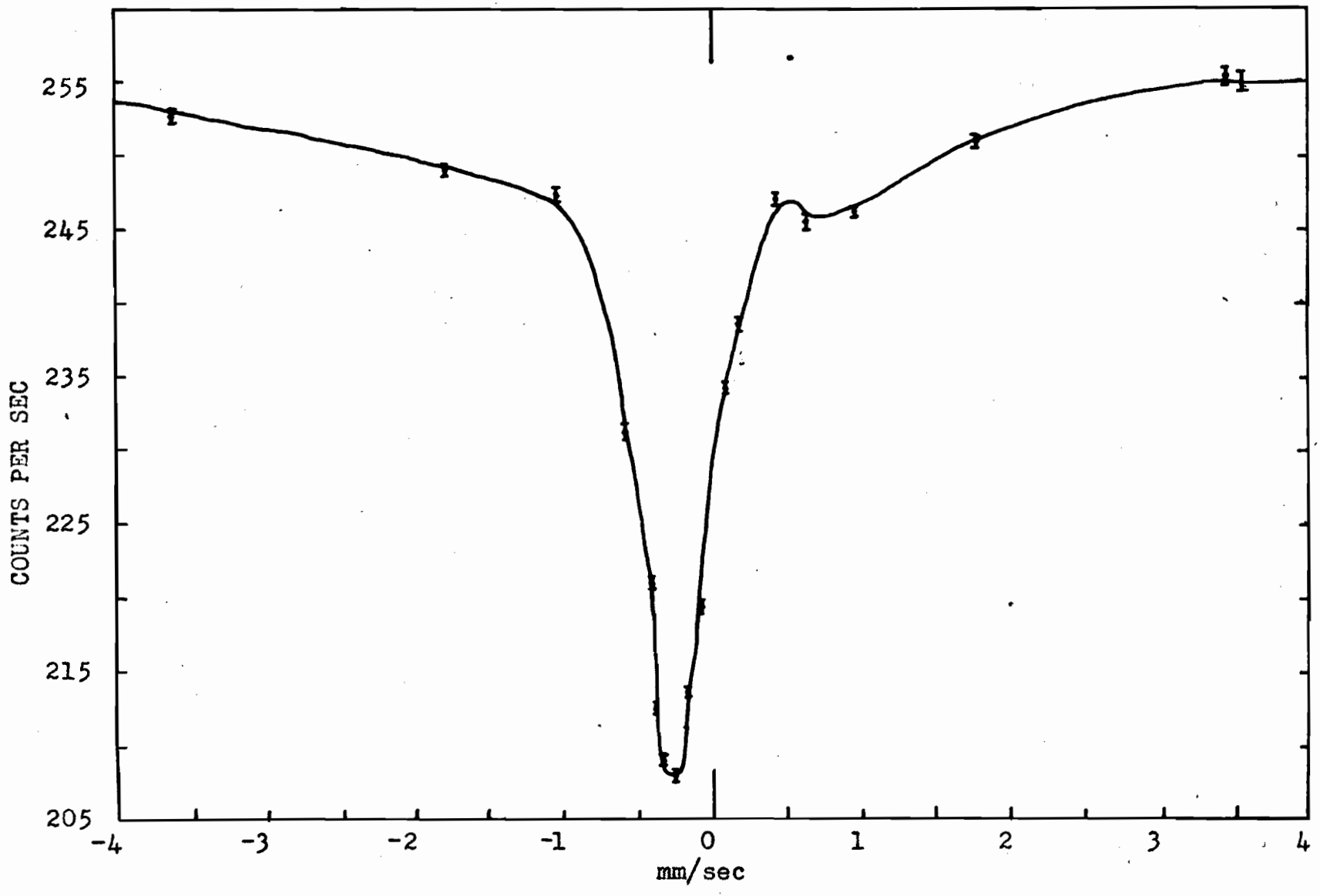

FIGURE 4-2 SOURCE: Co^{57} IN COPPER; ABSORBER: 310 S.S. 0.001" THICK

the line-width as determined experimentally is slightly wider than the natural line-width.

The broadening could arise from the range of environments experienced by various Fe atoms in the alloy, magnetic hyperfine interactions, or quadrupole interactions. As the magnetic broadening would be temperature dependent (related to the spin relaxation time), experiments in which the temperature was varied could be used to indicate the magnitude of its effect.

A large displacement of the centroid of the resonance curve from zero velocity was found. As the source and absorber were at the same temperature (room temperature), the magnitude of the second-order Doppler shift was very small compared to the total displacement. The main cause of the displacement is the isomer shift (the source host lattice is copper and the absorber host lattice is 310 stainless steel). Since the isomer shift arises from the electrostatic interaction between the nuclear charge distribution and the electronic charge density at the nucleus, if the s-electron density is different for the source and absorber, and the nuclear charge radius different for the ground and excited states, the difference in isomer shifts can be observed. The negative shift of (0.30 ± 0.02)mm/sec indicates that the source has a greater transition energy than the absorber, since to get perfect overlap of the emission and absorption spectra, a negative Doppler shift had to be given to the source energy.

If the s-electron density at the nucleus is taken to be less for the copper source (because of shielding of the 3 s-electrons by the 3 d-electrons) than for the stainless steel absorber, a smaller nuclear charge radius for the excited state of Fe^{57} would produce a shift in the observed direction. This can be seen from an equation given by Walker et al [18]:

$$E_a - E_s = \frac{2}{5}\pi Z e^2 \left[R_{is}^2 - R_{gr}^2\right]\left[|\Psi(0)_a|^2 - |\Psi(0)_s|^2\right] \quad (4\text{-}2)$$

where R_{is} and R_{gr} are the radii of the isomeric and ground states and $|\Psi(0)_a|^2$ and $|\Psi(0)_s|^2$ are the total s-electron densities of the nucleus for absorber and source respectively.

4.22 Cu Source and 310 Stainless Steel Absorber 0.00015 inch thick

The line-width of this curve (see Figure 4-3) is (0.45 ± 0.05)mm/sec, which gives, using equation (4-1), an energy width of $(21.56 \pm 2.40)\times10^{-9}$ev. Therefore, the actual line-width of the curve is $\Gamma = (10.78 \pm 1.20)\times10^{-9}$ev.

Then, using equation (2-27) the mean lifetime of the excited state is found to be $\tau = (0.61 \pm 0.07)\times10^{-7}$sec.

The thinner absorber results in a smaller change in the counting rate. The 0.001 inch thick absorber gives a 18.5% change, whereas the 0.00015 inch thick absorber gives a 4.6% change. This is due to the lower number of Fe^{57} atoms available for resonance absorption in the thin absorber.

The isomer shift is exactly the same for the thin absorber as for the thick absorber. This is as it should be, for the two absorbers present the same host lattice environment to the Fe^{57} nucleus.

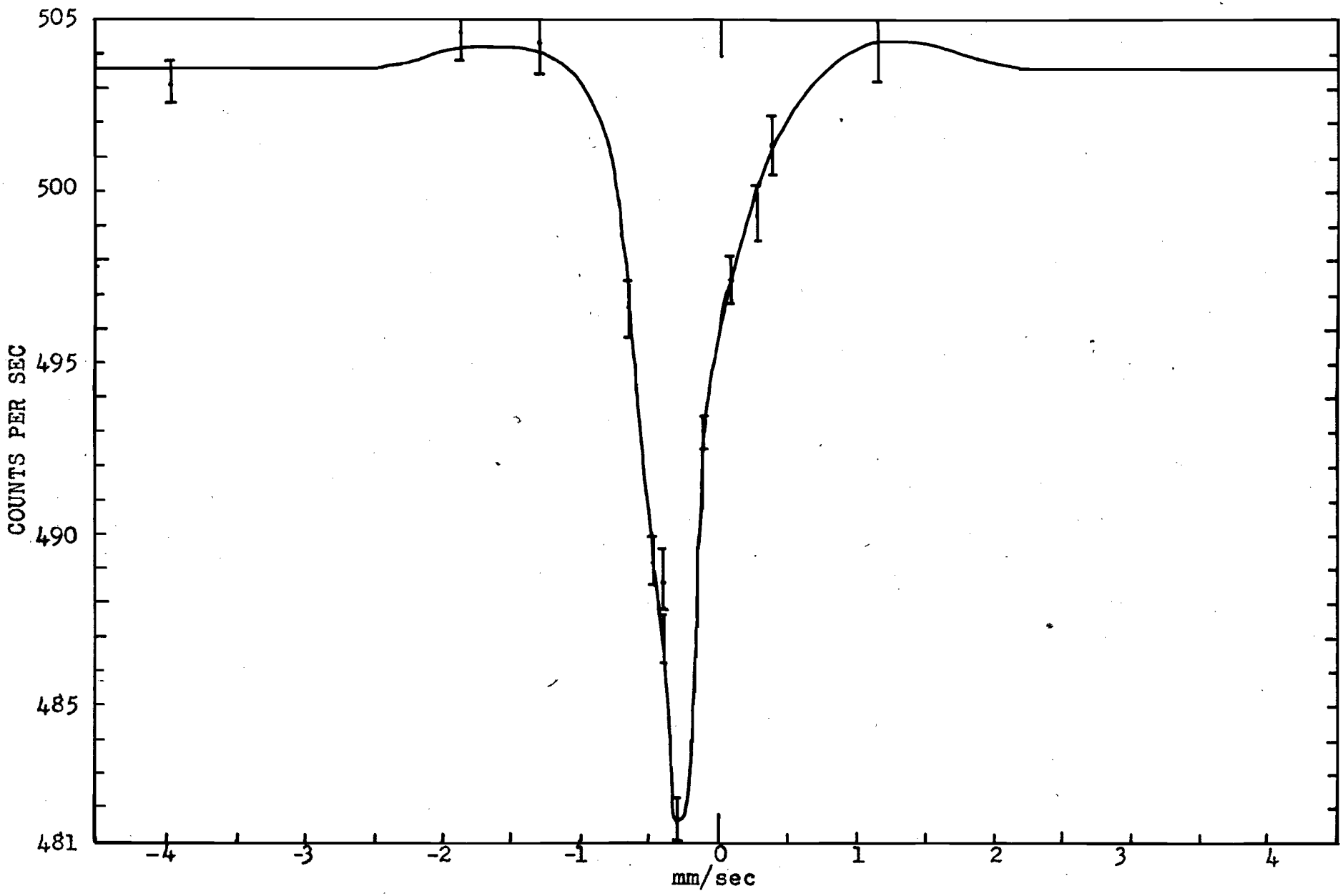

FIGURE 4-3 SOURCE: Co^{57} IN COPPER; ABSORBER: 310 S.S. 0.00015" THICK

4.23 310 Stainless Steel Source and 310 Stainless Steel Absorber 0.001 inch thick.

The line-width of this curve (see Figure 4-4) is (0.60 ± 0.05)mm/sec., which, in energy units, is $(28.74\pm2.40)\times10^{-9}$ ev. The actual line-width is therefore $\Gamma = (14.37\pm1.20)\times10^{-9}$ev.

The mean lifetime of the excited state is then found to be $\tau = (0.46\pm0.04)\times10^{-7}$sec.

G. K. Wertheim[17] has shown that there is an indication of temperature dependence in the line-width. This dependence would indicate magnetic hyperfine interaction broadening, which is dependent on the spin correlation time. This mechanism is probably the main contribution to the broadened line-width, together with the range of environments of the Fe^{57} nuclei, and the absorber thickness broadening.

The displacement of the centroid of the resonance curve from zero velocity is zero. Since the source and absorber host lattices are the same, and are at the same temperature, the second-order Doppler shift, and the difference in isomer shifts are both zero.

4.24 310 Stainless Steel Source and 310 Stainless Steel Absorber 0.00015 inch thick

The line-width of this curve (see Figure 4-5) is the same as that for the curve in section (4.23). Therefore the actual line-width and the mean lifetime are also the same.

The thin absorber results in a change in counting rate of 6.3% whereas the thicker absorber results in a change of

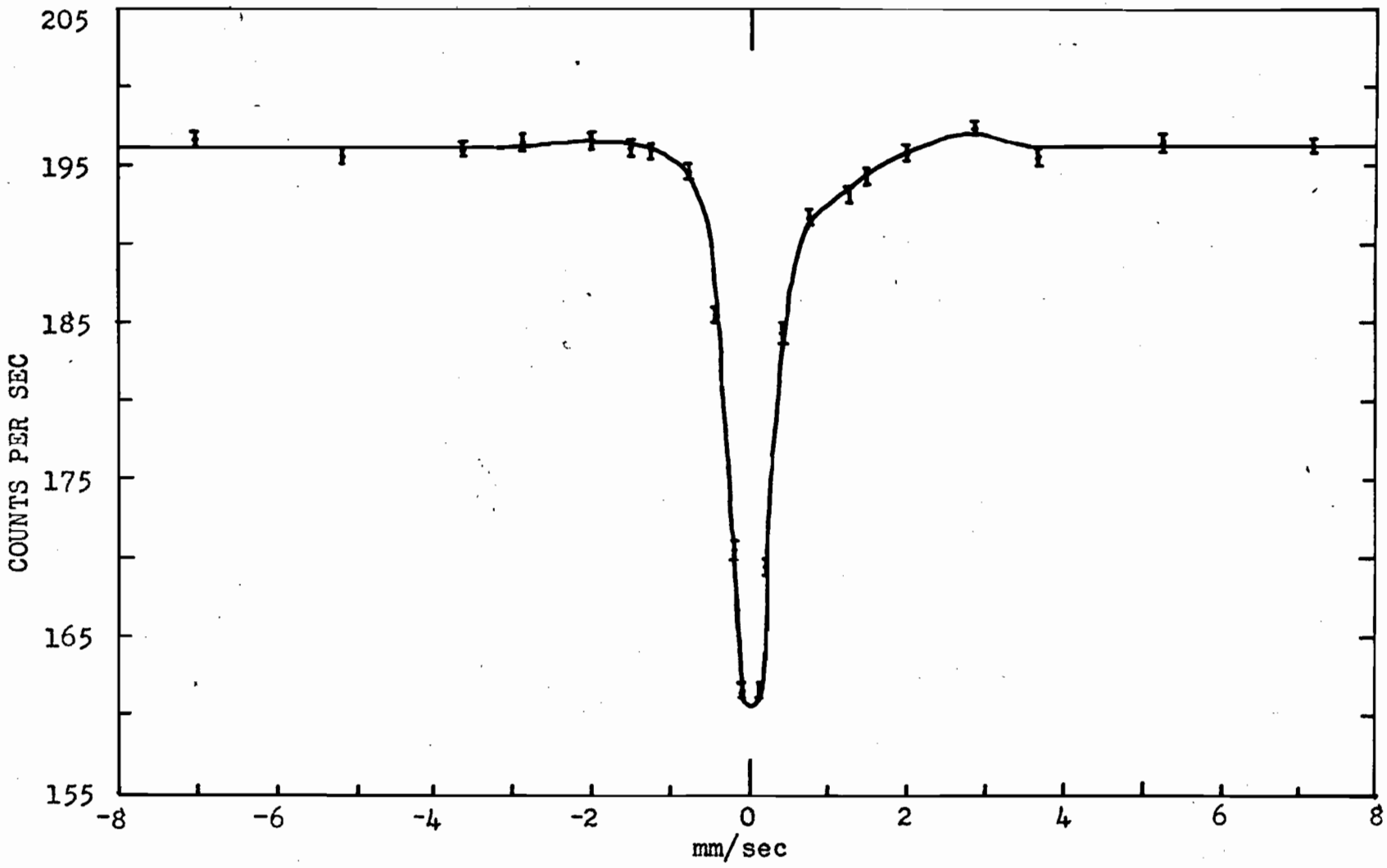

FIGURE 4-4 SOURCE: Co^{57} IN 310 S.S.; ABSORBER: 310 S.S. 0.001" THICK

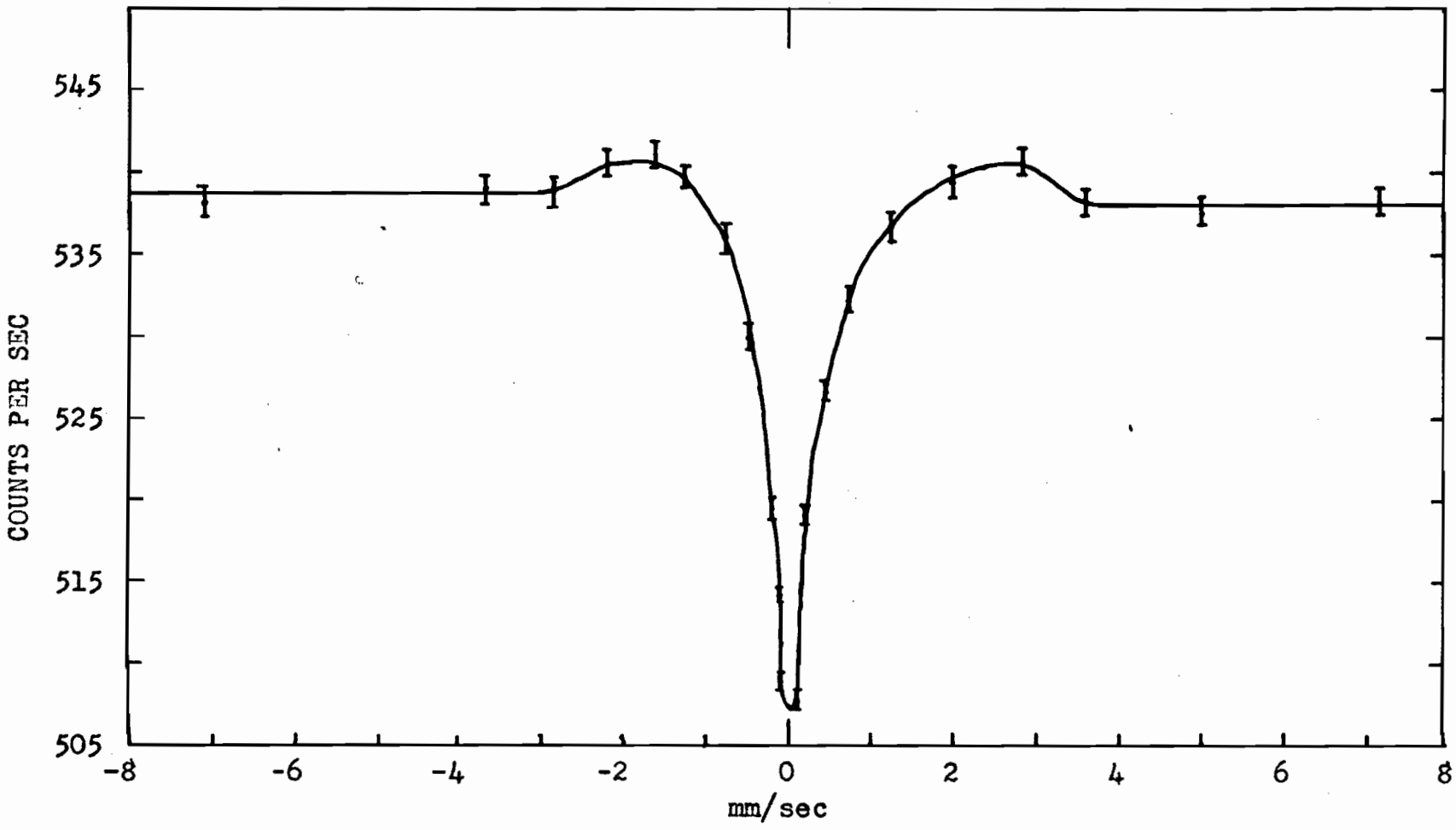

FIGURE 4-5 SOURCE: Co^{57} IN 310 S.S.; ABSORBER: 310 S.S. 0.00015" THICK

18.1%, as expected. The displacement of the resonance curve is zero, as the source and absorber are of the same material.

4.3 THE HYPERFINE SPECTRA

The Mössbauer source used here, Fe^{57}, is itself ferromagnetic. Therefore, hyperfine splitting can be observed by having Fe^{57} in an iron host lattice. The extreme narrowness of the line-width makes it possible to resolve these hyperfine splittings of the nuclear energy levels.

There are two basic combinations that can be used for studying hyperfine splittings: both source and absorber may be split, or only one of them. Although both methods have been used successfully, the combination of unsplit source with split absorber is preferable, as then complicated resonance patterns arising from the overlap of two multi-line spectra are avoided (overlap of any emission line-width with any absorption line will give resonance absorption).

In this section two combinations of split emission and absorption spectra and six combinations of unsplit emission or absorption spectra and split absorption or emission spectra are studied.

4.31 Fe Source and Natural Fe Absorber

Since the source and absorber host lattices are the same, there will be no significant differences between the positive and negative velocity results. Therefore, only the positive direction results are considered here (see Figure 4-6).

This combination has split emission and absorption spectra. There are six resolvable resonance lines for a one-

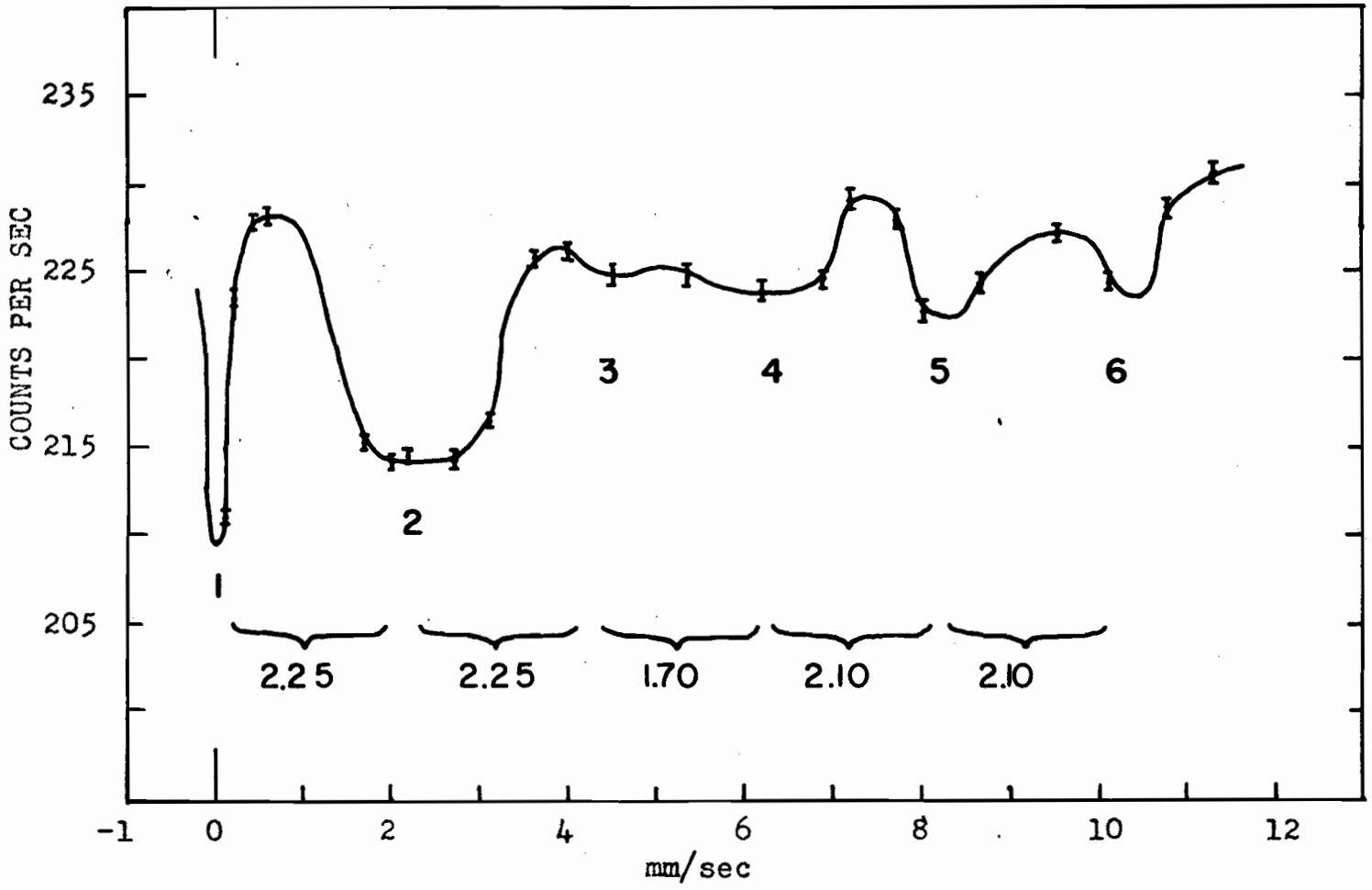

FIGURE 4-6 SOURCE: Co^{57} IN Fe; ABSORBER: NATURAL Fe

direction pattern. By applying an external magnetic field, Hanna et.al.[19] polarized the resonance radiation and thus showed that two unresolved doublets exist. The resolved lines are numbered from one to six in Figure 4-6. Line (2) is a doublet, however one of the members of the doublet is too weak to affect the position of the line. Line (3) is also a doublet, with both members fairly strong, so that the line position detected could be shifted.

Knowledge of the ground state spin of Fe^{57} makes possible an explanation of the hyperfine spectrum (see Figure 4-7).

The spacing between lines (1) and (2), (4) and (5), and (5) and (6) in Figure 4-6 should be equal to the splitting of the excited state. The spacing between lines (2) and (3) is not used because line (3) is actually a doublet. The spacing between lines (2) and (4) should be equal to the splitting of the ground state.

A small instability in the counting and detecting circuit has resulted in a slightly irregular resonance pattern. As a result, the spacings between (1) and (2), (4) and (5), and (5) and (6) are not equal. Since the spacings should be equal, the mean value will be used in calculations. It can be seen from Figure 4-6 that the mean spacing between lines (1) and (2),(4) and (5), and (5) and (6) is (2.15 ± 0.20)mm/sec. Then, by using equation (4-1), the excited state energy splitting of $(1.03 \pm 0.10) \times 10^{-7}$ev is obtained. The spacing between lines

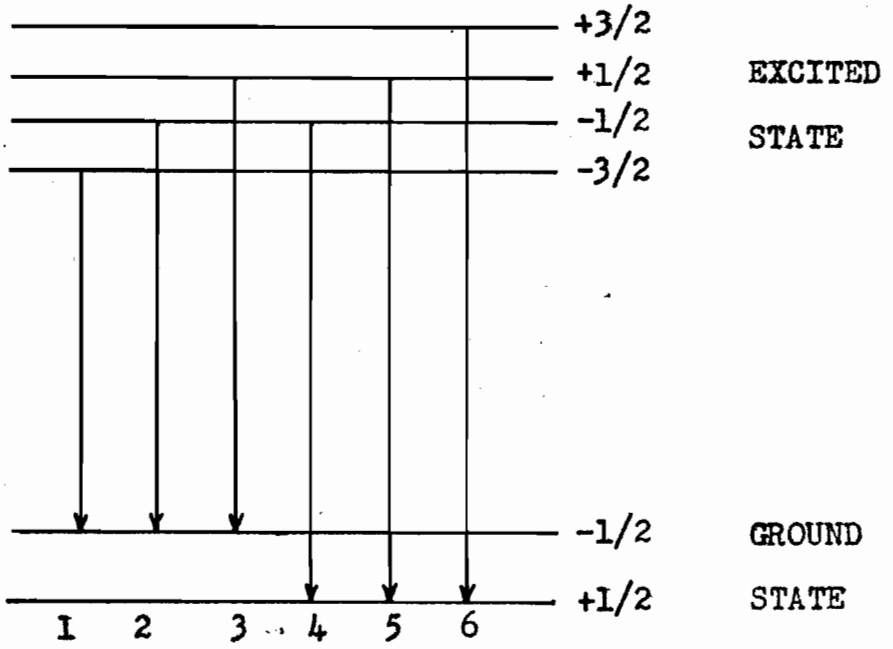

FIGURE 4-7 LEVEL DIAGRAM OF Fe^{57}

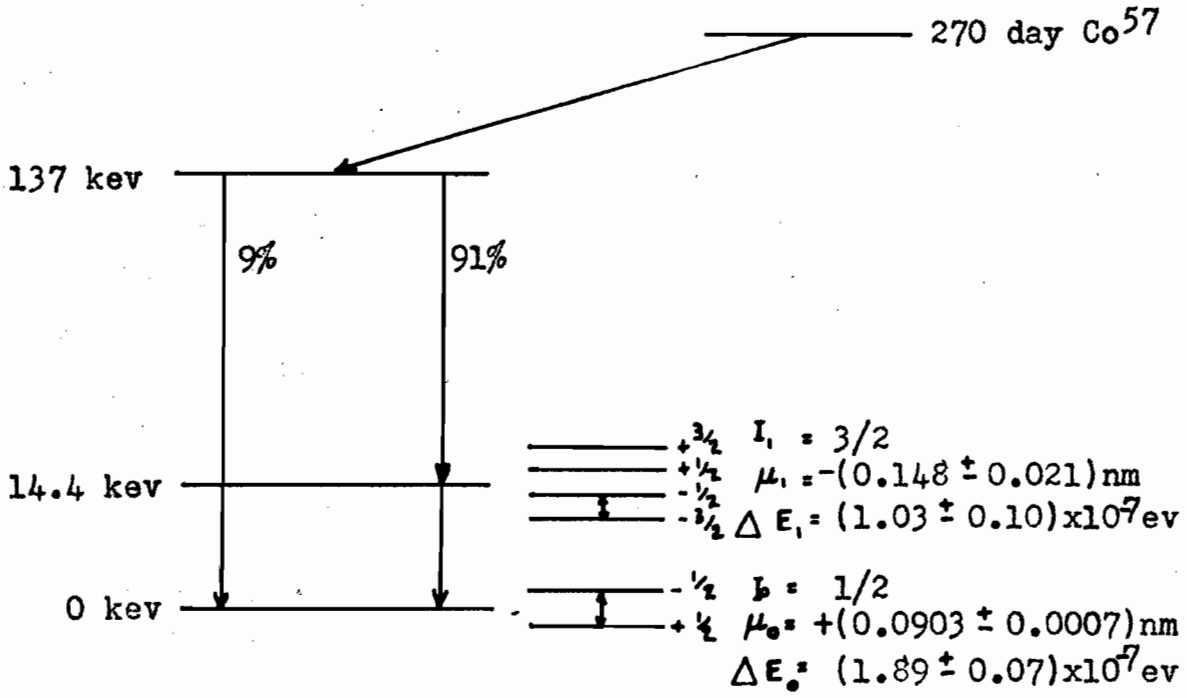

FIGURE 4-8 DETAILED DECAY SCHEME OF Fe^{57}

(2) and (4) is found to be (3.95 ± 0.15)mm/sec, giving a ground state energy splitting of $(1.89\pm0.07)\times10^{-7}$ev.

In order to calculate the internal field, equation (2-30) is used $$\Delta E = -m_I g_I H \qquad (2\text{-}30)$$

Here, ΔE will be taken as the ground state splitting, and m_I as Δm_I. The magnetic moment of the ground state of Fe^{57} has been accurately determined by Ludwig and Woodbury[20] to be $\mu_0 = +(0.0903\pm0.0007)$nm. For the ground state $I=\frac{1}{2}$ and $g_I = \mu_0/I = 0.1806$nm. Also, one nuclear magneton equals 0.315×10^{-11}ev/gauss. Substituting these values into equation (2-30) gives an internal field of $H = (3.32\pm0.15)\times10^5$ oersteds. Equation (2-30) is also used to obtain the magnetic moment of the excited state. This time ΔE is taken as the excited state splitting, $I = \frac{3}{2}$, $H = 3.32\times10^5$oe, and μ_1 is unknown. Substitution of the appropriate values into equation (2-30) yields an excited state magnetic moment of $\mu_1 = -(0.148\pm0.021)$nm. The interpretation of the hyperfine spectrum (see Figure 4-7) requires that the signs of the excited and ground state magnetic moments be opposite. Only if the signs of either the excited state magnetic quantum numbers or the ground state magnetic quantum numbers are reversed will the signs of the magnetic moments be the same.

Figure 4-8 shows the complete decay scheme of Fe^{57}, possible now that the energy splittings are known.

4.32 Fe Source and Enriched Fe^{57} Absorber.

This combination also has split emission and absorption spectra (see Figure 4-9). By increasing the number of stable

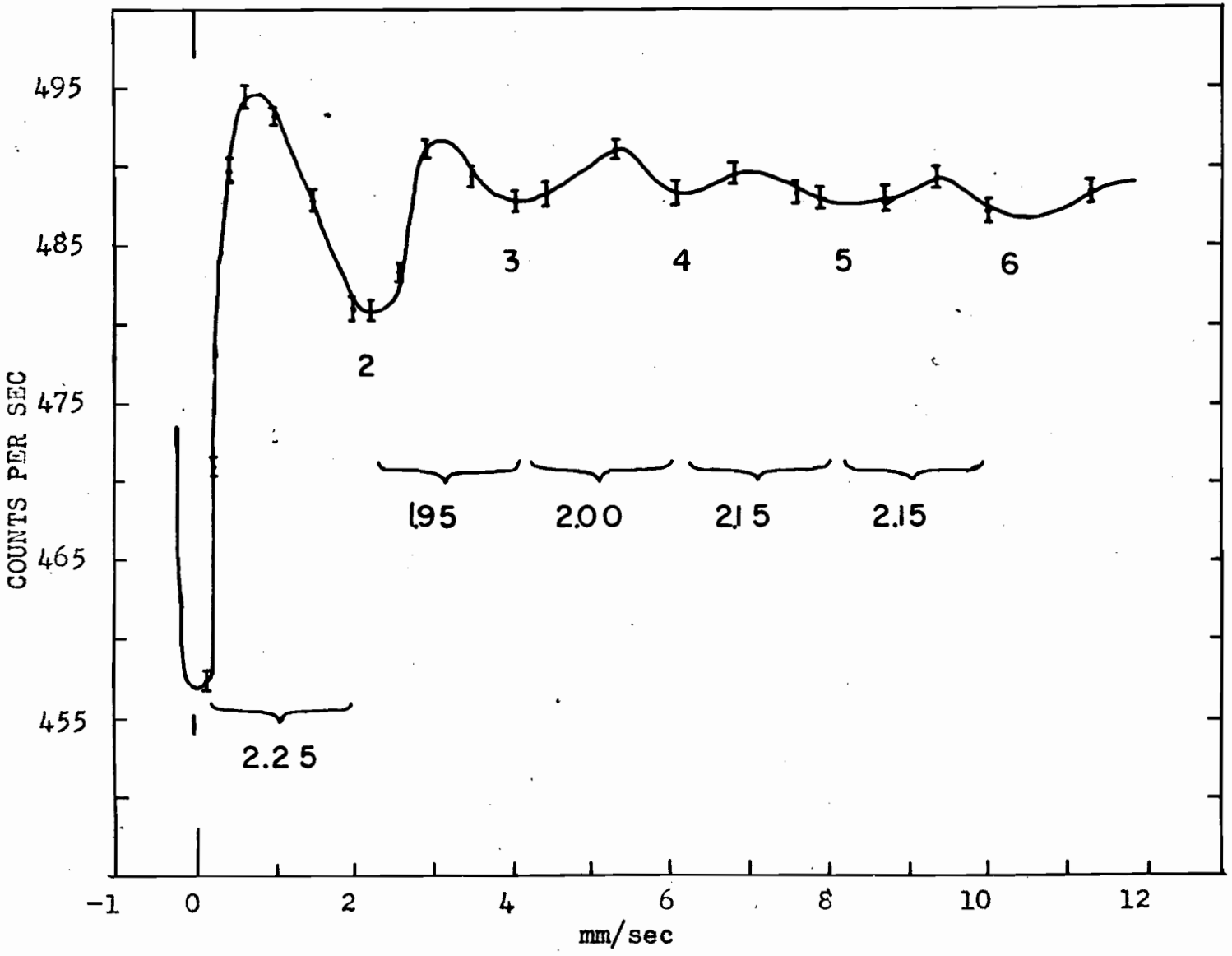

FIGURE 4-9 SOURCE: Co^{57} IN Fe; ABSORBER: ENRICHED Fe^{57}

isotope nuclei in the absorber, greater resonance absorption is possible and a more clearly defined resonance pattern is obtained. As in the case of section (4.31) only the positive direction results are considered here.

The mean value of the spacing between lines (1) and (2), (4) and (5), and (5) and (6) is (2.18 ± 0.10) mm/sec. therefore, the excited state energy splitting is $(1.04 \pm 0.05) \times 10^{-7}$ ev. The spacing between lines (2) and (4) is found to be (3.95 ± 0.10)mm/sec., giving a ground state energy splitting of $(1.89 \pm 0.05) \times 10^{-7}$ev.

Again, using equation (2-30), and internal field of $H = (3.32 \pm 0.11) \times 10^{5}$ oersteds is obtained. Similarly, the magnetic moment of the excited state is found to be $\mu_1 = -(0.149 \pm 0.012)$nm.

The results obtained in this section, and in section (4.31) are very similar, as they should be, for the only difference between them is the density of Fe^{57} in the absorber. Also, these results are in very good agreement with Hanna et al [19] results of $(3.33 \pm 0.10) \times 10^{5}$ oersteds for the internal field and $-(0.153 \pm 004)$nm for the magnetic moment of the excited state.

4.33 Cu Source and Natural Fe Absorber

This combination has a split absorption spectrum, but it has an unsplit emission spectrum. As a result, the resonance pattern is much simpler, consisting of a total of six resonance lines for a pattern including positive and

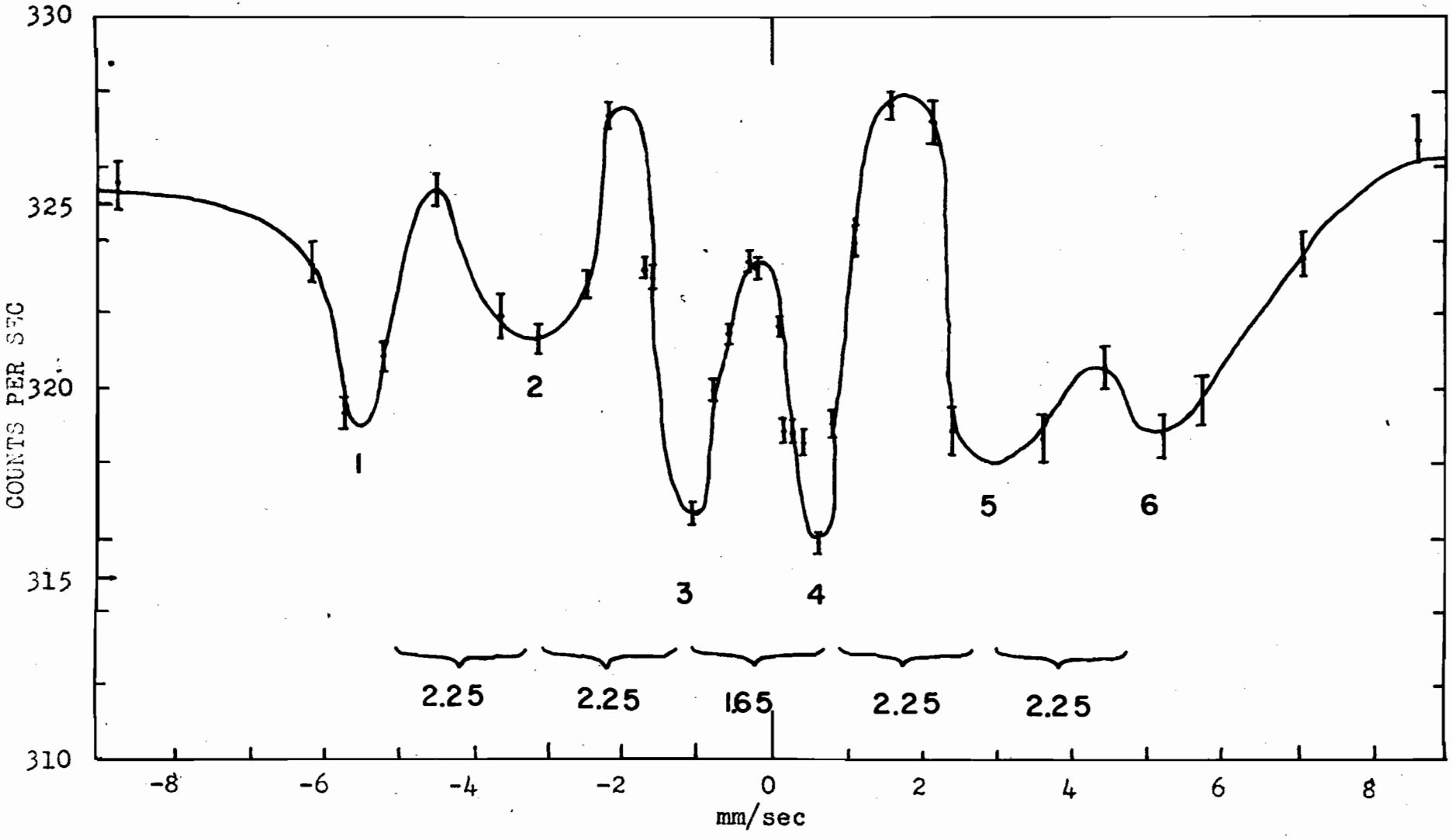

FIGURE 4-10 SOURCE: Co^{57} IN COPPER; ABSORBER: NATURAL Fe

negative velocities (see Figure 4-10). Both positive and negative velocity results must be included because of the isomer shift between the copper source and iron absorber. The centroid of the resonance pattern is displaced minus (0.20 ± 0.05)mm/sec.

The spacing between lines (1) and (2), (4) and (5), and (5) and (6) still gives the excited state splitting, but now the spacing between lines (2) and (3) also does, because line (3) is no longer a doublet. Similarly, the spacing between lines (2) and (4) still gives the ground state splitting, but now the spacing between lines (3) and (5) also does. The spacing between lines (1) and (2), (2) and (3), (4) and (5), and (5) and (6) is equal in this resonance pattern. This spacing of (2.25 ± 0.10)mm/sec. yields an excited state energy splitting of $(1.08 \pm 0.05) \times 10^{-7}$ ev. The spacing between lines (2) and (4), and (3) and (5) is (3.90 ± 0.10) mm/sec., giving a ground state energy splitting of $(1.87 \pm 0.50) \times 10^{-7}$ ev.

Using equation (2-30) in the same manner as that in section (4.31), an internal field of $H = (3.29 \pm 0.11) \times 10^{5}$ oersteds is obtained. Similarly, the magnetic moment of the excited state is found to be $-(0.156 \pm 0.013)$nm.

4.34 Cu Source and Enriched Fe^{57} Absorber

This combination has a split absorption spectrum and an unsplit emission spectrum. As can be seen in Figure 4-11, the use of an enriched absorber increases the sharpness of the resonance peaks.

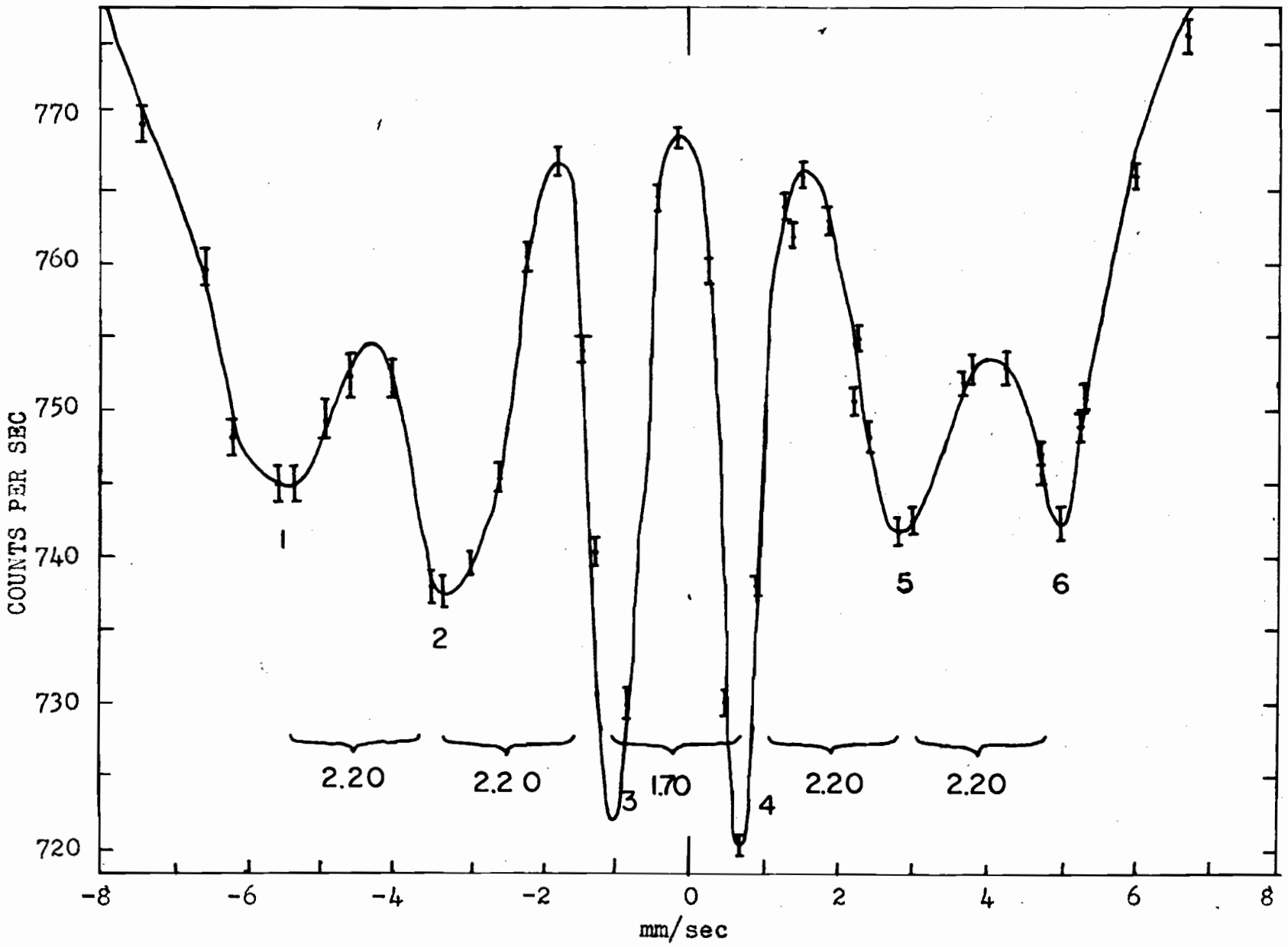

FIGURE 4-11 SOURCE: Co^{57} IN COPPER; ABSORBER: ENRICHED Fe^{57}

The spacing between lines (1) and (2), (2) and (3), (4) and (5), and (5) and (6) is (2.20 ± 0.05)mm/sec, yielding an excited state energy splitting of $(1.05 \pm 0.02) \times 10^{-7}$ev. The spacing between lines (2) and (4), and (3) and (5) is (3.90 ± 0.05)mm/sec., giving a ground state energy splitting of $(1.87 \pm 0.02) \times 10^{-7}$ ev.

From equation (2-30), the internal field is found to be $(3.29 \pm 0.06) \times 10^{5}$ oersteds. The excited state magnetic moment is $-(0.152 \pm 0.006)$nm.

The results obtained in this section and in section (4.33) are very similar, as the absorbers are almost the same, and the sources are the same. The results are close to those obtained by Hanna et al.[19] The internal field obtained here is slightly less than that for the Fe source - Fe absorber combination.

4.35 310 Stainless Steel Source and Natural Fe Absorber

This combination also has a split absorption spectrum and an unsplit emission spectrum. The resonance pattern (see Figure 4-12) is similar to that in sections (4.33) and (4.34), consisting of six resonance lines. The resonance pattern is not symmetric due to a slight counting instability. There is a small isomer shift of plus (0.10 ± 0.05)mm/sec.

The spacing between lines (1) and (2), (2) and (3), (4) and (5), and (5) and (6) is (2.10 ± 0.15)mm/sec., yielding an excited state energy splitting of $(1.01 \pm 0.07) \times 10^{-7}$ ev. The spacing between lines (2) and (4), and (3) and (5) is (3.80 ± 0.10) mm/sec., giving a ground state energy splitting of $(1.82 \pm 0.05) \times 10^{-7}$ ev.

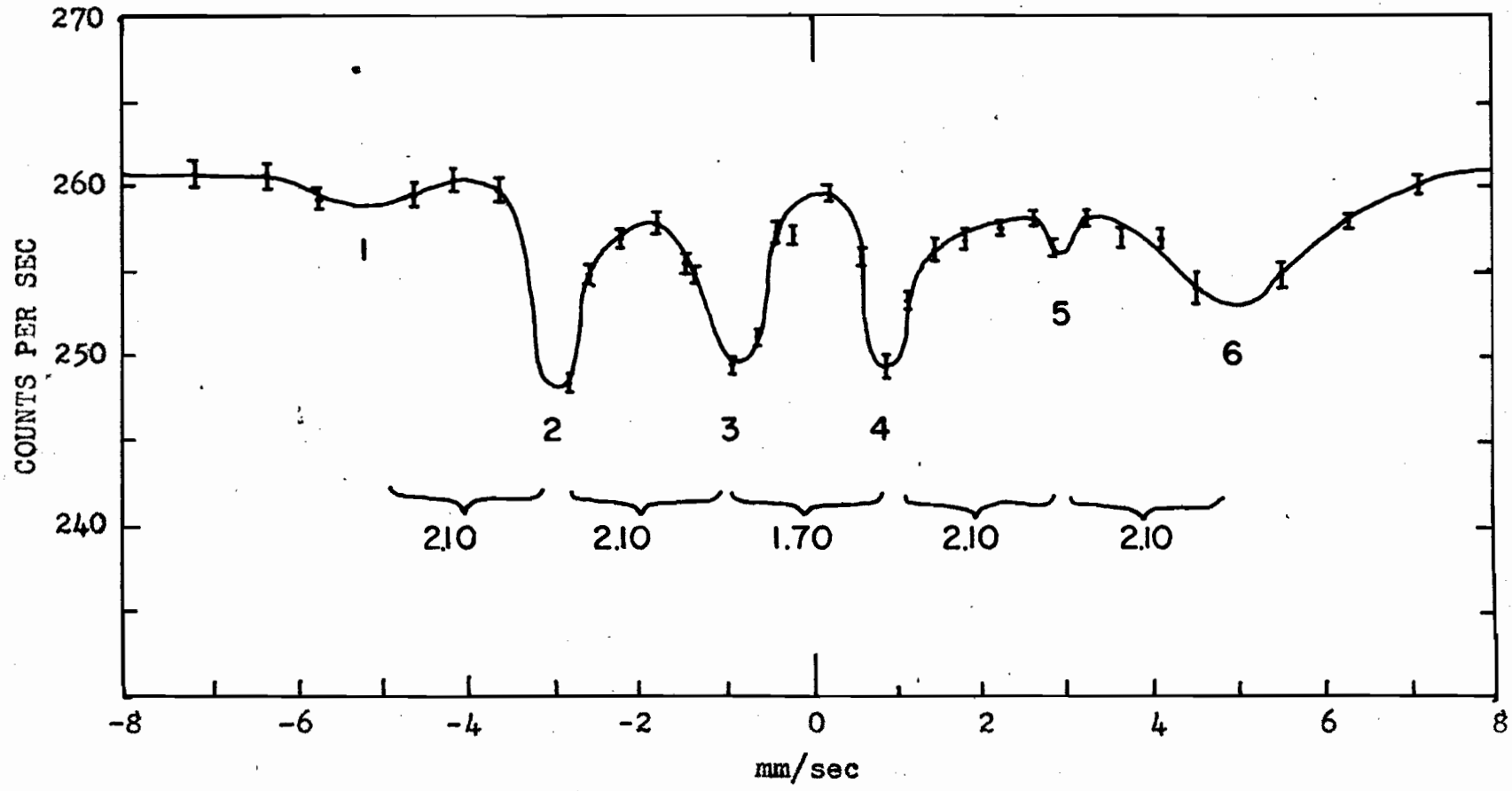

FIGURE 4-12 SOURCE: Co^{57} IN 310 S.S.; ABSORBER: NATURAL Fe

The internal field is found to be $(3.20\pm0.11)\times10^5$ oersteds, and the magnetic moment of the excited state is $-(0.150\pm0.016)$nm.

4.36 310 Stainless Steel Source and Enriched Fe^{57} Absorber

A more sharply defined resonance pattern has been obtained by using the enriched absorber (see Figure 4-13).

The spacings are exactly the same as for the natural Fe absorber, resulting in the same internal field and magnetic moment of the excited state. As the pattern is more sharply defined, the uncertainty of the peak positions is smaller. The excited state energy splitting is $(1.01\pm0.02)\times10^{-7}$ev and the ground state energy splitting is $(1.82\pm0.02)\times10^{-7}$ ev. The internal field is found to be $(3.20\pm0.06)\times10^5$ oersteds, and the magnetic moment of the excited state is $-(0.150\pm0.006)$nm.

4.37 Fe Source and 310 Stainless Steel Absorber 0.001 inch thick

This combination has a split emission spectrum and an unsplit absorption spectrum (see Figure 4-14). A decrease in the Mössbauer effect will occur with this combination, for now the emitted gamma rays have six energies. Therefore, at any specific resonance, only a fraction of the emitted rays will be resonantly absorbed. A counting instability caused the resonance pattern to be unsymmetric.

The spacing between lines (1) and (2), (2) and (3), (4) and (5), and (5) and (6) is (2.30 ± 0.25)mm/sec, giving an excited state energy splitting of $(1.10\pm0.12)\times10^{-7}$ev. The spacing between lines (2) and (4), and (3) and (5) is (4.00 ± 0.20)mm/sec, giving a ground state energy splitting of $(1.92\pm0.10)\times10^{-7}$ ev.

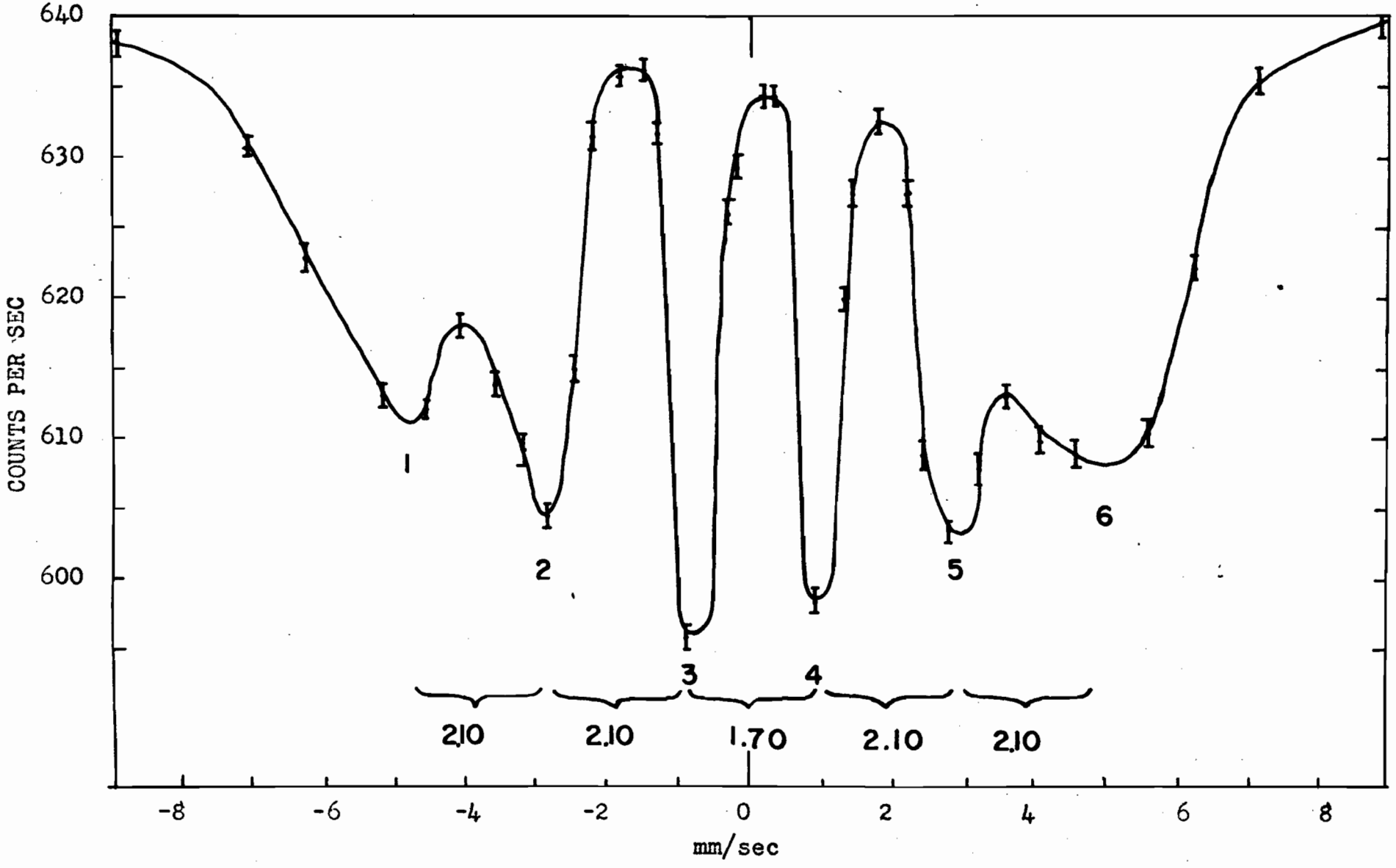

FIGURE 4-13 SOURCE: Co^{57} IN 310 S.S.; ABSORBER: ENRICHED Fe^{57}

The internal field is found to be $(3.38\pm0.20)\times10^{5}$ oersteds and the magnetic moment of the excited state is $-(0.155\pm0.026)$nm.

4.38 Fe Source and 310 Stainless Steel Absorber 0.00015 inch thick

This combination also results in a reduced Mössbauer effect (see Figure 4-15). Again, counting instability has caused an unsymmetric pattern.

The mean spacing between lines (1) and (2), (2) and (3), (4) and (5), and (5) and (6) is (2.13 ± 0.20)mm/sec, giving an excited state energy splitting of $(1.02\pm0.10)\times10^{-7}$ev. The mean spacing between lines (2) and (4), and (3) and (5) is $3.80\pm0.15)$mm/sec, giving a ground state energy splitting of $(1.82\pm0.07)\times10^{-7}$ev.

The internal field is found to be $(3.20\pm0.15)\times10^{5}$ oersteds and the magnetic moment of the excited state is $-(0.152\pm0.022)$nm.

The value of the internal field as obtained in section (4.37), and that obtained in this section should be almost the same, as only the absorber thickness was changed. There is, however a difference. Counting instability and the small Mössbauer effect resulted in difficulty in establishing the exact location of the resonance lines, and it is probably these two factors which contribute most to the difference in values.

A summary of all the results is presented in Table 4.1.

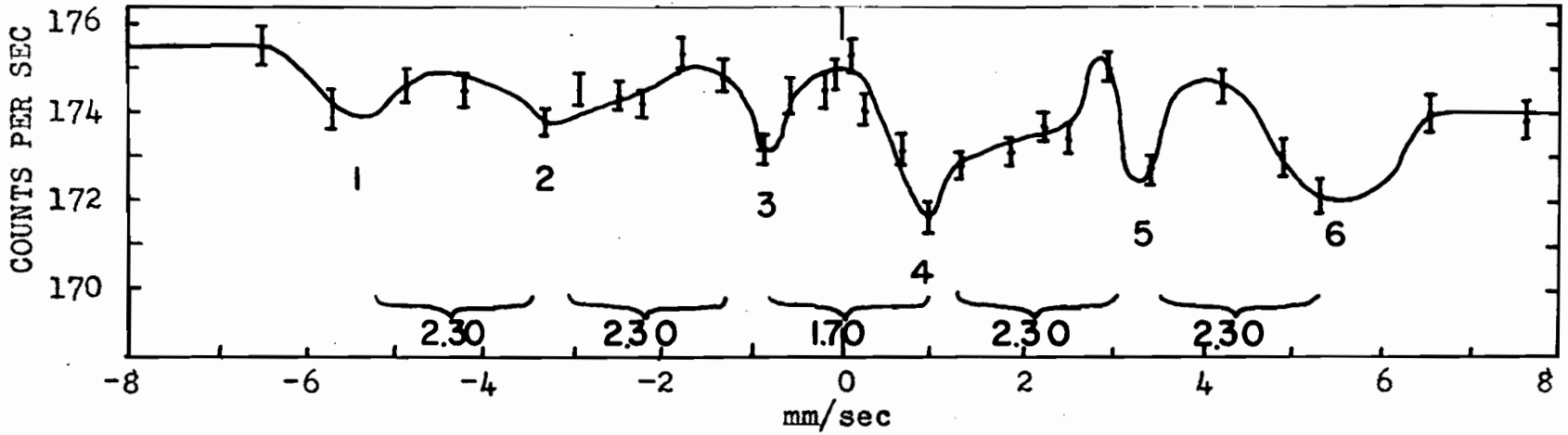

FIGURE 4-14 SOURCE: Co^{57} IN Fe; ABSORBER: 310 S.S. 0.001" THICK

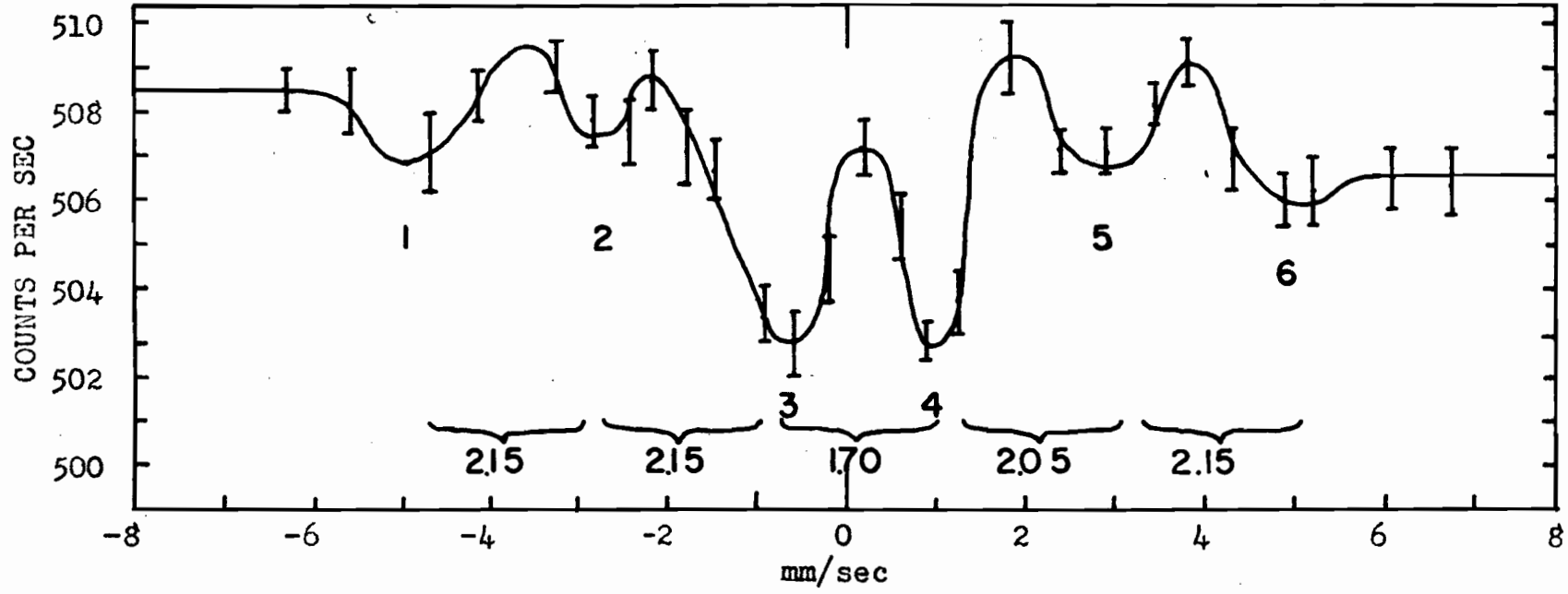

FIGURE 4-15 SOURCE: Co^{57} IN Fe; ABSORBER: 310 S.S. 0.00015" THICK

TABLE 4.1 SUMMARY OF RESULTS

Source	Absorber	Absorber Thickness (inches)	Line-width	Mean Lifetime (10^{-7} sec)	Isomer Shift (mm/sec)
Cu	310 s.s.	0.001	13.18 ± 1.20	0.50 ± 0.04	-0.30 ± 0.02
Cu	310 s.s.	0.00015	10.78 ± 1.20	0.61 ± 0.07	-0.30 ± 0.02
310s.s.	310 s.s.	0.001	14.37 ± 1.20	0.46 ± 0.04	0
310s.s.	310 s.s.	0.00015	14.37 ± 1.20	0.46 ± 0.04	0

Source	Absorber	Absorber Thickness (inches)	Excited State Splitting (10^{-7} ev)	Ground State Splitting (10^{-7} ev)	Internal Field (10^{5} oe)	Magnetic Moment of Excited State (nm)
Fe	Nat.Fe	0.001	1.03 ± 0.10	1.89 ± 0.07	3.32 ± 0.15	-0.148 ± 0.021
Fe	Enr.Fe^{57}	0.0001	1.04 ± 0.05	1.89 ± 0.05	3.32 ± 0.11	-0.149 ± 0.012
Cu	Nat.Fe	0.001	1.08 ± 0.05	1.87 ± 0.05	3.29 ± 0.11	-0.156 ± 0.013
Cu	Enr.Fe^{57}	0.0001	1.05 ± 0.02	1.87 ± 0.02	3.29 ± 0.06	-0.152 ± 0.006
310 s.s.	Nat.Fe	0.001	1.01 ± 0.07	1.82 ± 0.05	3.20 ± 0.11	-0.150 ± 0.016
310 s.s.	Enr. Fe^{57}	0.0001	1.01 ± 0.01	1.82 ± 0.02	3.20 ± 0.06	-0.150 ± 0.006
Fe	310 s.s.	0.001	1.10 ± 0.12	1.92 ± 0.10	3.38 ± 0.20	-0.155 ± 0.026
Fe	310 s.s.	0.00015	1.02 ± 0.10	1.82 ± 0.07	3.20 ± 0.15	-0.152 ± 0.022
Mean Value			1.04 ± 0.07	1.86 ± 0.05	3.28 ± 0.12	-0.152 ± 0.015

CHAPTER V

CONCLUSIONS

Apparatus has been designed and constructed which detects the Mössbauer effect in Fe^{57} at room temperature. This effect has been studied in detail with various source and absorber combinations in order to gain information about certain solid-state properties, and experience for future work with the effect. In addition, the theory of the Mössbauer effect is reviewed.

Measurements of the mean lifetime of the first excited state of Fe^{57} were made and it was found to be at least $(0.61\pm0.07)\times10^{-7}$ secs.

The isomer shift has been explained, and measured. A shift of $-(0.30\pm0.02)$mm/sec. was obtained for the copper source - 310 stainless steel absorber combination, thus indicating that this source has a greater transition energy than the absorber. That the nuclear charge radius was smaller for the excited state of Fe^{57} than for the ground state of Fe^{57} was also shown as a result of the detected isomer shift.

The hyperfine structure of Fe^{57} was studied, and the spectrum explained. The splitting of the first excited state of Fe^{57} was shown to have a mean value of $(1.04\pm0.07)\times10^{-7}$ev. The ground state splitting was shown to have a mean value of $(1.86\pm0.05)\times10^{-7}$ ev.

The internal field at the iron nucleus is found to have a mean value of $(3.28 \pm 0.12) \times 10^5$ oersteds.

The magnetic moment of the first excited state of Fe^{57} was shown to have a mean value of $-(0.152 \pm 0.015)$nm.

The source and absorber combinations that give the most clearly defined Mössbauer effect were found. To study the hyperfine structure of Fe^{57}, a Cu source and an enriched Fe^{57} absorber, or a 310 stainless steel source and an enriched Fe^{57} absorber will give the sharpest resonance peaks.

Considerable experience has been obtained in detection of the Mössbauer effect by use of the constant velocity method. The disadvantages of this method are thus well known. Any drift or discontinuity in the counting and detection systems will be applied only to the point being studied at that moment. If a change in counting rate occurs, the position of one of the hyperfine resonance peaks may be seriously affected, or even a false one created (or an actual peak missed). This method requires at least two days to obtain an unsplit resonance curve, and three days to obtain a hyperfine spectrum. During this time, any counting rate drift will, at least, cause the pattern to be unsymmetric, and possibly affect the position of the peaks. The detector circuit has been found to be quite temperature dependent, so that a constant temperature environment is required for these long term experiments.

The velocity sweep method, on the other hand, yields a complete resonance pattern quickly. Any change in counting rate is distributed along the whole pattern so that the peaks are not shifted, created, or missed. As a result, patterns obtained by this method can be considered more reliable. Despite the considerable cost of a multichannel analyzer, the velocity sweep method is strongly recommended for any future research.

The resonance radiation in the case of Fe^{57} is quite low in energy (14.4 kev.). A thin Na I(Tl) scintillation counter was used here, however, a gas-filled proportional counter would provide better resolution of this radiation against background.

Vibration of the apparatus proved not as important as was originally thought. A combination of lead weights and rubber mounts effectively damped out vibrations so that a considerable Mössbauer effect was detected.

In addition to the experiments which were conducted to gain experience and information about the Mössbauer effect in Fe^{57} for future research, a visit was made (Dec. 1963) to the Brookhaven National Laboratory, and discussionswere held with B. Mozer, P.P. Craig, and O.C. Kistner. These discussions confirmed the above conclusion that the multichannel analyzer velocity sweep method was a necessity for more refined applications of the Mössbauer effect.

Discussions with B. Mozer on his application

of the effect to the study of localized lattice vibrations around a light impurity atom, a study which was planned for this laboratory, revealed that a considerable amount of special equipment would be required, and that the probability of success was only marginal.

P.P. Craig discussed the possibility of studying the spin relaxation time by examining the hyperfine structure as a function of concentration and temperature. This experiment also involves a considerable amount of equipment, but the probability of success is much greater.

In the main, the discussions at Brookhaven pointed out that future solid-state research by application of the Mössbauer effect would require a considerable amount of relatively expensive equipment, and a number of specially prepared sources and absorbers. Taking the various above factors into consideration, an experiment involving localized lattice vibrations cannot be presently recommended.

In conclusion, the research undertaken here has shown how the Mössbauer effect can be detected and applied to obtain information about the mean lifetime of the first excited state of Fe^{57}, the isomer shift, the internal magnetic field at the iron nucleus, and the magnetic moment of the first excited state of Fe^{57}. This exploratory research has also demonstrated that future work with the Mössbauer effect would require substantial financial involvement.

REFERENCES

1. R. L. Mössbauer, Z. Physik, 151, 124 (1958)
2. P. B. Moon, Proc. Phys. Soc. A, 64, 76, (1951)
3. C.P. Swan and F. R. Metzger, Phys. Rev., 108, 982, (1957)
4. K. G. Malmfors, Ark. Fysik, 6, 49, (1952)
5. W. E. Lamb, Jr., Phys. Rev., 55, 190, (1939)
6. H. Frauenfelder, The Mössbauer Effect, W.A. Benjamin, Inc., New York, U.S.A., (1962)
7. L.I. Schiff, Quantum Mechanics, Secs. 23 and 35, McGraw-Hill, New York, U.S.A., (1955)
8. H. J. Lipkin, Annals of Physics, 9, 194, (1960)
9. B.D. Josephson, Phys. Rev. Letters, 4, 341, (1960)
10. O.C. Kistner and A.W. Sunyar, Phys. Rev. Letters, 4, 412, (1960)
11. A.J.F. Boyle and H. E. Hall, Reports Prog. Phys. XXV, 504, (1962)
12. R. Barlautaud and C. Tzara, Phys. Rev. Letters, 4, 405, (1960)
13. H. Frauenfelder, D.R.F. Cochran, D.E. Nagle, and R.D. Taylor, Nuovo Cimento, 19, 183, (1961)
14. E. Kankeleit, Z. Physik, 164, 442, (1961)
15. K.P. Mitrofanov and V.S. Shpinel, Soviet Physics JETP, 13, 686, (1961)
16. J. G. Dash, R.D. Taylor, D.E. Dash, P.P. Craig, and W.M. Visscher, Phys. Rev., 122, 1116, (1961).
17. G.K. Wertheim, J. Appl. Phys. (suppl), 32,110S. (1961)
18. L. R. Walker, G.K. Wertheim and V. Jaccarins, Phys. Rev. Letters, 6, 98, (1961)
19. S.S. Hanna, J. Heberle, C.L. Littlejohn, G.J. Perlow, R.S. Preston, and D.H. Vincent, Phys. Rev. Letters, 4, 177, (1960)
20. G.W. Ludwig and H. H. Woodbury, Phys. Rev., 117, 1286, (1960).

21. G. K. Wertheim and J.H. Wernick, Phys. Rev., 123, 755, (1961)

22. J. van Kranendonk, W. Low and P.P. Craig, Proceedings of the Seventh International Conference on Low Temperature Physics, University of Toronto Press, Toronto, (1961)

23. W.M. Visscher, Annals of Physics, 9, 194, (1960)

24. R. Bauminger, S.G. Cohen, A. Marinov, and S. Ofer, Phys. Rev., 122, 743, (1961)

25. R.E. Watson and A.J. Freeman, Phys. Rev., 123, 2027, (1961)

26. A.A. Maradudin, P.A. Flinn, and S. Ruby, Phys. Rev., 126, 9, (1962)

27. R.V. Pound and G.A. Rebka, Jr., Phys. Rev. Letters, 3, 544, (1959)

28. J.P. Schiffer and W. Marshall, Phys. Rev. Letters, 3, 556, (1959)

29. G. De Pasquali, H. Frauenfelder, S. Margulies, and R.N. Peacock, Phys. Rev. Letters, 4, 71, (1960)

30. S.S. Hanna, J. Heberle, C. Littlejohn, G.J. Perlow, R. S. Preston, and D.H. Vincent, Phys. Rev. Letters, 4, 28, (1960)